Polymer 236 (2021) 124304

Contents lists available at ScienceDirect

Polymer

journal homepage: www.elsevier.com/locate/polymer

Formulation based predictive cure kinetics modelling of epoxy resins

Gabriele Voto [a,b,*], Leela Sequeira [b], Alexandros A. Skordos [a]

[a] Cranfield University, School of Aerospace, Transport and Manufacturing, Enhanced Composites and Structures Centre, Cranfield, MK43 0AL, United Kingdom
[b] Hexcel Composites Ltd, R&T AeroMatrix and Adhesive, Duxford, CB22 4QB, United Kingdom

ARTICLE INFO

Keywords:
Composite matrices
Matrix composition design
Formulation Ratio Superposition
Thermosetting resin
Amine curative
Cure kinetics
Process modelling
Composites manufacturing

ABSTRACT

Matrix formulation for aero-grade high-performance carbon fibre reinforced thermoset composites is a challenging task relying on extensive knowledge of chemistry, legacy information and trial-and-error iterations to identify a suitable pre-polymer resin/curative combination. This work proposes the development and application of a cure kinetics methodology to tailor preliminary matrix formulations focusing on matrix constituents reactivity. The kinetics of a ternary system containing either one epoxy pre-polymer and two amine curatives or two epoxy pre-polymers and one amine curative is approximated as a linear combination of the kinetics of its elementary binary systems containing the corresponding epoxy pre-polymer and amine curative. The method has been evaluated on a wide range of epoxy/amine formulations and shown to be valid with a reaction rate error lower than 0.003 min^{-1}. The application of this predictive method allows the design of matrix systems with tailored reactivity and cure time without extensive experimentation.

1. Introduction

Epoxy resins are a well-established class of polymeric thermosetting materials due to their versatility, property stability and processability which have made their application possible to a wide range of products as coatings, structural adhesives and composite matrices [1–3]. The market success of epoxies has been driven by the continuous innovation in the synthesis of new raw materials aimed to improve performance and by the flexibility offered in customising their processing conditions.

Different epoxy pre-polymers are available depending on their method of synthesis, physiochemical properties and final end-user application with bisphenolic, novolac and multifunctional epoxies the most widely used types in industry [2,3]. Epoxy pre-polymers react with a large variety of curative agents [3–5] such as aromatic amines and anhydrides, which are ideal for high-performance applications due to the superior characteristics and processing temperatures of the corresponding formulations. Adjusting the epoxy pre-polymer(s)/curative(s) relative composition allows to tailor the material to meet required mechanical and functional properties. However, success in this task relies on the ability to understand the cure reaction and to balance the required properties by judicious selection of possible constituents within a large portfolio of potential choices.

Currently, there is no standard procedure to facilitate the screening of candidate chemicals to be used in a matrix formulation. Decisions on class, combination and processing conditions of the matrix constituents rely on legacy information, historical data and experimental iterations. This makes the design of matrix formulations time-consuming and cost-intensive. The development of matrix systems with higher reactivity, lower reaction enthalpy, faster manufacturability and reduced exothermic risk is receiving greater attention as composite technologies are nowadays challenged to demonstrate robustness towards high-rate industrialisation scenarios and process sustainability with the aerospace industry leading these developments [6–8]. Novel composite materials and processes must be proven to be high-performance, scalable, flexible, cost-effective and fit for digitisation. This highlights the need to identify efficient and unbiased approaches to develop the next generation of thermosetting epoxy matrices; in this perspective, the utilisation of predictive material models would help to progress from traditional strategies, saving on development time needed to optimise the matrix formulations and associated process parameters.

Matrix cure kinetics modelling has been used to represent the reaction rate of polymeric matrices. Phenomenological approaches [9–39] have represented a solid alternative to mechanistic models [40–54] as they do not require a priori knowledge of the matrix reaction mechanisms. Assuming the matrix reaction rate is a unique function of temperature and degree of cure, they are based on empirical equations

* Corresponding author. Cranfield University, School of Aerospace, Transport and Manufacturing, Enhanced Composites and Structures Centre, Cranfield, MK43 0AL, United Kingdom.
E-mail address: G.Voto@cranfield.ac.uk (G. Voto).

https://doi.org/10.1016/j.polymer.2021.124304
Received 6 May 2021; Received in revised form 19 October 2021; Accepted 24 October 2021
Available online 26 October 2021

Table 1
Selected chemicals.

Chemical	Symbol	Molecular weight (g/mol)	Chemical structure	Equivalent weight (g/eq)	
				Epoxy	Amine hydrogen
TGPAP	E_1	277.31	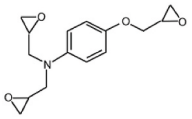	100.0	–
TGDDM	E_2	422.52	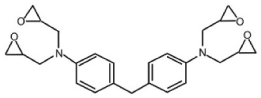	113.0	–
3,3′ DDS	X_1	248.30	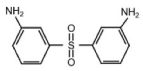	–	63.0
4,4′ DDS	Y_1	248.30	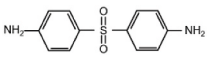	–	63.0
M-MIPA	X_2	310.48	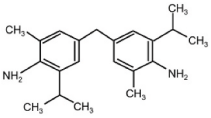	–	77.6
M-CDEA	Y_2	379.37	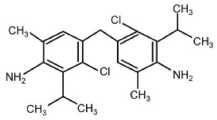	–	94.8
PES	TP	232.26	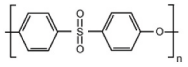	–	–

resembling chemical kinetics without necessarily corresponding to the chemical reaction equation of the system. The general form of these models is:

$$\frac{d\alpha}{dt} = f(T, \alpha) \tag{1}$$

The implementation of phenomenological models requires experimental tests usually run through differential scanning calorimetry (DSC) and numerical determination of the kinetics parameters of the selected equation through curve fitting. This approach yields robust models, yet specific to the fully formulated matrix system. This makes the investment in resources required for developing a detailed cure kinetics model relevant only once the formulation has been established commercially. Therefore, cure kinetics is neglected during the initial stage of resin development. This results in missed opportunities as the huge variety of commercial pre-polymers and curatives could offer alternative matrix formulations which meet better process efficiency targets. A parametric connection between matrix chemistry and associated reaction rate factoring in the reactive functional group fractions has the potential to overcome current limitations in the design of matrix formulations taking kinetics into consideration.

This work aims to facilitate epoxy matrix formulation through the development and application of a cure kinetics model which, in contrast to state-of-the-art phenomenological methodologies, focuses on the matrix constituent content to approximate predictively the cure process. The proposed modelling methodology uses linear superposition of the kinetics of two-component formulations to approximate the reaction behaviour of more complex three-component systems. A few superposition theories [55–58] have been applied in the context of composites manufacturing in the past. However, these are not based on a matrix constituent parameterisation and do not consider a modular matrix formulation. The proposed approach is tested here on a large variety of amine/epoxy matrices to assess validity over a range of different molecular weights and functionalities.

2. Materials and methods

2.1. Raw materials

High-performance thermosetting epoxy pre-polymers and aromatic amine curatives were investigated in this work to cover a wide spectrum of applications to aerospace composite matrices. Tri-glycidyl-p-aminophenol (TGPAP) and N,N,N′,N′-tetra-glycidyl-4,4′—diaminodiphenylmethane (TGDDM) were the two selected epoxies, whilst 3,3′-diaminodiphenylsulfone (3,3′ DDS), 4,4′-diaminodiphenylsulfone (4,4′ DDS), 4,4′-methlylenebis(2-isopropyl-6-methylaniline) (M-MIPA) and 4,4′-methlylenebis(3-chloro-2,6-diethylaniline) (M-CDEA) were the four aromatic amines used. Also polyethersulfone (PES) was selected as thermoplastic toughener. Table 1 details the selected chemicals, their molecular weight, chemical structure and epoxy or amine hydrogen equivalent weight as well as the nomenclature used.

2.2. Developmental matrix systems

The constituents were mixed both in binary and ternary combinations; binary blends were made of basic pre-polymer/amine pairs, whilst ternary materials were made of either one pre-polymer and two amines or vice versa spanning different fractions of the reacting constituent functional groups. This resulted in twenty-seven matrix blends arranged in five developmental matrix sets. All blends were based on a stoichiometric ratio as follows:

$$r = \frac{\sum_i \left(\frac{m_{A_i}}{AHEW_i}\right)}{\sum_i \left(\frac{m_{E_i}}{EEW_i}\right)} \tag{2}$$

where r is the amine/resin ratio imposed to be one, EEW_i, $AHEW_i$ are the i-th epoxy and amine hydrogen equivalent weight respectively and m_{E_i}, m_{A_i} are the i-th epoxy and amine mass respectively. The ternary blends were designed so that a fraction of each amine (or epoxy) completely reacts with the epoxy (or amine) while preserving a stoichiometric

Table 2
Binary and ternary formulations.

Group	Matrix	Mass fractions							Functional group fractions			
		E_1	E_2	X_1	X_2	Y_1	Y_2	TP	f_1^e	f_2^e	f_1^c	f_2^c
TGPAP/DDS	$E_1^{100}X_1^{100}$	0.61	–	0.39	–	–	–	–	1	–	1	–
	$E_1^{100}Y_1^{100}$	0.61	–	–	–	0.39	–	–	1	–	–	1
	$E_1^{100}X_1^{50}Y_1^{50}$	0.61	–	0.195	–	0.195	–	–	1	–	0.5	0.5
	$E_1^{100}X_1^{20}Y_1^{80}$	0.61	–	0.08	–	0.31	–	–	1	–	0.2	0.8
	$E_1^{100}X_1^{40}Y_1^{60}$	0.61	–	0.16	–	0.23	–	–	1	–	0.4	0.6
	$E_1^{100}X_1^{70}Y_1^{30}$	0.61	–	0.27	–	0.12	–	–	1	–	0.7	0.3
	$E_1^{100}X_1^{90}Y_1^{10}$	0.61	–	0.35	–	0.04	–	–	1	–	0.9	0.1
MULTF/33DDS	$E_1^{100}X_1^{100}$	0.61	–	0.39	–	–	–	–	1	–	1	–
	$E_2^{100}X_1^{100}$	–	0.64	0.36	–	–	–	–	–	1	1	–
	$E_1^{50}E_2^{50}X_1^{100}$	0.29	0.34	0.37	–	–	–	–	0.5	0.5	1	–
TGPAP/LNZ	$E_1^{100}X_2^{100}$	0.56	–	–	0.44	–	–	–	1	–	1	–
	$E_1^{100}Y_2^{100}$	0.51	–	–	–	–	0.49	–	1	–	–	1
	$E_1^{100}X_2^{50}Y_2^{50}$	0.54	–	–	0.21	–	0.25	–	1	–	0.5	0.5
	$E_1^{100}X_2^{20}Y_2^{80}$	0.52	–	–	0.08	–	0.40	–	1	–	0.2	0.8
	$E_1^{100}X_2^{40}Y_2^{60}$	0.53	–	–	0.17	–	0.30	–	1	–	0.4	0.6
	$E_1^{100}X_2^{70}Y_2^{30}$	0.55	–	–	0.30	–	0.15	–	1	–	0.7	0.3
	$E_1^{100}X_2^{90}Y_2^{10}$	0.56	–	–	0.39	–	0.05	–	1	–	0.9	0.1
TGDDM/DDS	$E_2^{100}X_1^{100}$	–	0.64	0.36	–	–	–	–	–	1	1	–
	$E_2^{100}Y_1^{100}$	–	0.64	–	–	0.36	–	–	–	1	–	1
	$E_2^{100}X_1^{50}Y_1^{50}$	–	0.64	0.18	–	0.18	–	–	–	1	0.5	0.5
	$E_2^{100}X_1^{20}Y_1^{80}$	–	0.64	0.07	–	0.29	–	–	–	1	0.2	0.8
	$E_2^{100}X_1^{40}Y_1^{60}$	–	0.64	0.14	–	0.22	–	–	–	1	0.4	0.6
	$E_2^{100}X_1^{70}Y_1^{30}$	–	0.64	0.25	–	0.11	–	–	–	1	0.7	0.3
	$E_2^{100}X_1^{90}Y_1^{10}$	–	0.64	0.32	–	0.04	–	–	–	1	0.9	0.1
TGPAP/DDS/TP	$E_1^{100}X_1^{100}TP$	0.51	–	0.32	–	–	–	0.17	1	–	1	–
	$E_1^{100}Y_1^{100}TP$	0.51	–	–	–	0.32	–	0.17	1	–	–	1
	$E_1^{100}X_1^{50}Y_1^{50}TP$	0.51	–	0.16	–	0.16	–	0.17	1	–	0.5	0.5

Notation: E_1:TGPAP; E_2:TGDDM; X_1:3,3′ DDS; X_2:M-MIPA; Y_1:4,4′ DDS; Y_2:M-CDEA; TP:PES.

Table 3
Autocatalytic cure kinetics parameters of binary systems.

Group	Matrix	**A**(1/min)	$\mathbf{E_{ACT}}$(J/mol)	**m**	**n**
TGPAP/DDS	$E_1^{100}X_1^{100}$	$1.0{\cdot}10^7$	$6.2{\cdot}10^4$	0.9	2.1
	$E_1^{100}Y_1^{100}$	$2.9{\cdot}10^7$	$6.9{\cdot}10^4$	0.7	2.0
TGPAP/LNZ	$E_1^{100}X_2^{100}$	$4.6{\cdot}10^5$	$5.3{\cdot}10^4$	1.1	1.7
	$E_1^{100}Y_2^{100}$	$4.9{\cdot}10^4$	$5.0{\cdot}10^4$	1.0	1.5
TGDDM/DDS	$E_2^{100}X_1^{100}$	$1.2{\cdot}10^7$	$6.6{\cdot}10^4$	0.7	1.1
	$E_2^{100}Y_1^{100}$	$1.0{\cdot}10^8$	$7.7{\cdot}10^4$	0.5	1.0
TGPAP/DDS/TP	$E_1^{100}X_1^{100}TP$	$6.1{\cdot}10^6$	$6.2{\cdot}10^4$	0.9	1.6
	$E_1^{100}Y_1^{100}TP$	$9.8{\cdot}10^6$	$6.5{\cdot}10^4$	1.0	2.2

amine/epoxy ratio for the whole blend.

The epoxy matrix systems were classified into five groups: (i) TGPAP/DDS which includes tri-functional TGPAP pre-polymer (E_1) with 3,3′ DDS (X_1) and 4,4′ DDS (Y_1) curing agents; (ii) MULTF/33DDS which includes tri-functional TGPAP (E_1) and tetra-functional TGDDM (E_2) pre-polymers with 3,3′ DDS (X_1) curing agent; (iii) TGPAP/LNZ which involves TGPAP pre-polymer (E_1) with M-MIPA (X_2) and M-CDEA (Y_2) curing agents; (iv) TGDDM/DDS which involves tetra-functional TGDDM pre-polymer (E_2) with 3,3′ DDS (X_1) and 4,4′ DDS (Y_1) curing agents; and (v) TGPAP/DDS/TP which is an extension of the TGPAP/DDS systems to include PES soluble thermoplastic. Table 2 reports the component mass fractions and the corresponding reactive functional group fractions f_i^j (with $i = 1, 2$; $j = e, c$ for epoxy or amine) for all blends. The notation used for each matrix blend indicates the constituents and functional fractions, e.g. $E_1^{100}X_1^{70}Y_1^{30}$ corresponds to 100% TGPAP epoxy with 70% of the total amine reactive sites contributed by 3,3′ DDS and 30% of the total amine sites contributed by 4,4′ DDS.

The first two formulation groups (TGPAP/DDS and MULTF/33DDS) aim to assess the cure kinetics approach for combinations of one epoxy with two amines and of two epoxies with one amine. The third group (TGPAP/LNZ) is used to test the approach for combinations of constituents with a wider reactivity range and the fourth set (TGDDM/DDS) to investigate the behaviour of systems with constituents with a large reaction activation temperature difference. The fifth group (TGPAP/DDS/TP) extends the application of the approach to systems containing a thermoplastic modifier. The investigated range of matrix formulations includes wide variations in both molecular weight and functionality to challenge the proposed cure kinetics model.

2.3. Matrix cure kinetics experimental characterisation

A TA Instruments Discovery DSC was used to measure the heat released during the cure of matrix samples. The sample size used was about 2 mg (±10%). Hermetic aluminium pans and lids were used. Each test was run in a controlled inert atmosphere at 50 ml/min nitrogen gas flow. A single dynamic ramp at 1 °C/min from −20 °C to 350 °C and two isothermal tests at 160 °C and 180 °C were carried out for each blend; a

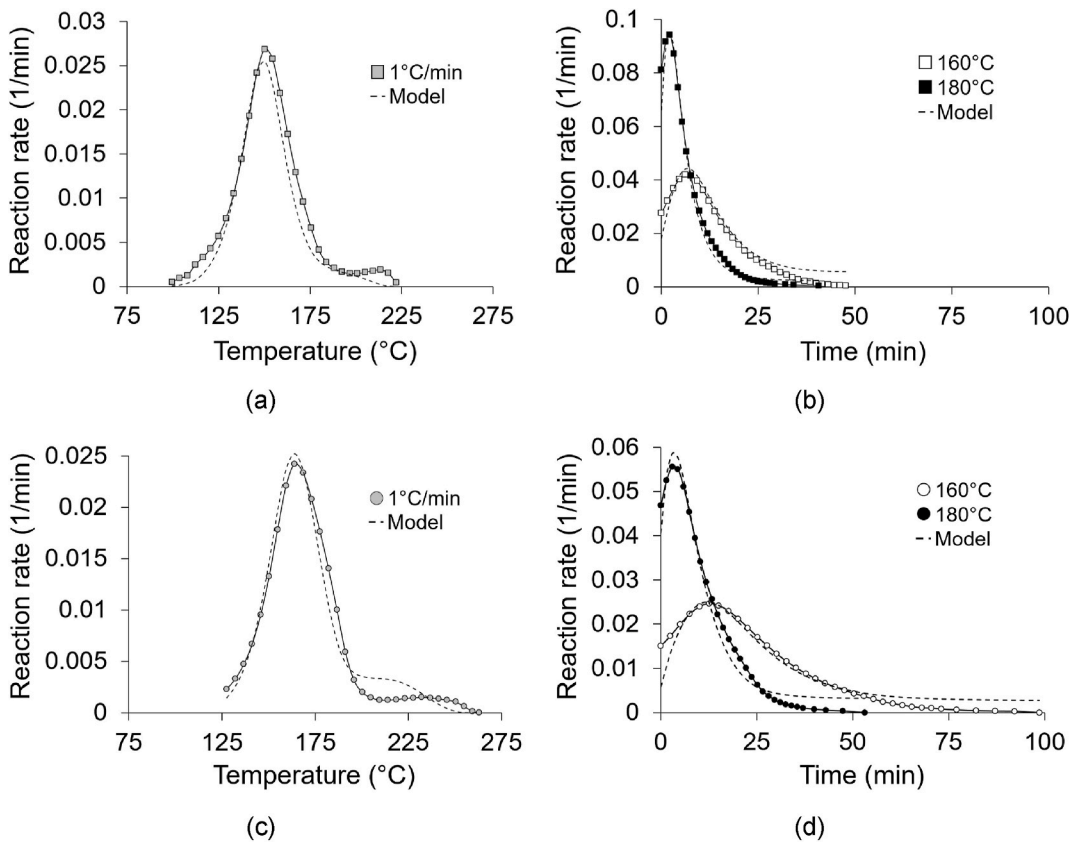

Fig. 1. Autocatalytic model fitting for the TGPAP/DDS group: (a) dynamic and (b) isothermal data for the $E_1^{100}X_1^{100}$ binary blend; (c) dynamic and (d) isothermal data for the $E_1^{100}Y_1^{100}$ binary blend.

20 °C/min heating ramp was applied to reach the isothermal test temperature, whilst the dwell duration ranged between 90 and 300 min depending on the amine/epoxy reactivity. The dynamic thermograms were integrated with an iterative baseline [59], whilst the isothermal curves with a horizontal baseline. The reaction rate results for each blend system obtained from dynamic and isothermal experiments were superimposed in a degree of cure-temperature space to verify no cure path dependence on the applied thermal history.

2.4. Formulation Ratio Superposition (FRS) cure kinetics modelling

Traditional phenomenological cure kinetics equations present intrinsic limitations in supporting the formulation of new polymeric matrices as they cannot take into account chemical composition modifications. The Formulation Ratio Superposition (FRS) approach presented in this work establishes a connection between matrix chemistry and cure modelling. The method focuses on the cure kinetics characterisation of the matrix binary constituents combined through a parameterisation of the constituent functional group fractions to predict the reaction behaviour of fully formulated ternary matrices. The model considers a unique value of the degree of conversion to account for concurrent and competitive reaction mechanisms.

In the case of one epoxy pre-polymer (E) and two amine curatives (X,Y), the reaction rate of a ternary matrix blend (EXY) is the weighted average of the reaction rates of its individual binary constituents (EX,EY) as follows:

$$\left.\frac{d\alpha}{dt}\right|_{EXY} = f_X^c \left.\frac{d\alpha}{dt}\right|_{EX} + f_Y^c \left.\frac{d\alpha}{dt}\right|_{EY} \tag{3}$$

where α is the matrix degree of conversion, $\frac{d\alpha}{dt}$ the reaction rate and f_X^c, f_Y^c the crosslink fractions contributed by each curing agent X,Y respectively.

In the case of autocatalytic kinetics [14–19] of each binary blend, Eq. (3) becomes:

$$\left.\frac{d\alpha}{dt}\right|_{EXY} = f_X^c A_{EX} e^{-\frac{E_{EX}}{RT}} \alpha^{m_{EX}} (1-\alpha)^{n_{EX}} + f_Y^c A_{EY} e^{-\frac{E_{EY}}{RT}} \alpha^{m_{EY}} (1-\alpha)^{n_{EY}} \tag{4}$$

where A_i is the pre-exponential factor, E_i the activation energy and m_i, n_i the reaction orders of each binary blend with $i = (EX,\ EY)$; T is the temperature in Kelvin and R the gas constant.

A single term autocatalytic model, such as the one used here, is the simplest choice for representing epoxy cure, whereas more complex models such as combined nth-order/autocatalytic kinetics or double autocatalytic kinetics yield a better representation including secondary mechanisms. This simplifying choice was made in this work to enable robust characterisation of the cure of the numerous binary systems examined to be carried out with an efficient testing campaign. Given the focus on assessing the FRS methodology, the representation of the main curing mechanism through the single autocatalytic model is sufficient to satisfy this aim. Furthermore, the single autocatalytic model has been used successfully to represent the curing of TGDDM\DDS-based epoxies [35,60], which are similar to formulations tested in this work.

Similarly, for one amine curative (X) and two epoxy pre-polymers (E_1,E_2), the reaction rate of a fully formulated ternary blend (E_1E_2X) is the weighted average of the reaction rates of its individual binary constituents (E_1X,E_2X) as follows:

$$\left.\frac{d\alpha}{dt}\right|_{E_1E_2X} = f_{E_1}^e \left.\frac{d\alpha}{dt}\right|_{E_1X} + f_{E_2}^e \left.\frac{d\alpha}{dt}\right|_{E_2X} \tag{5}$$

where $f_{E_1}^e$, $f_{E_2}^e$ are the crosslink fractions contributed by each E_1, E_2 pre-polymer respectively. For autocatalytic kinetics, Eq. (5) becomes:

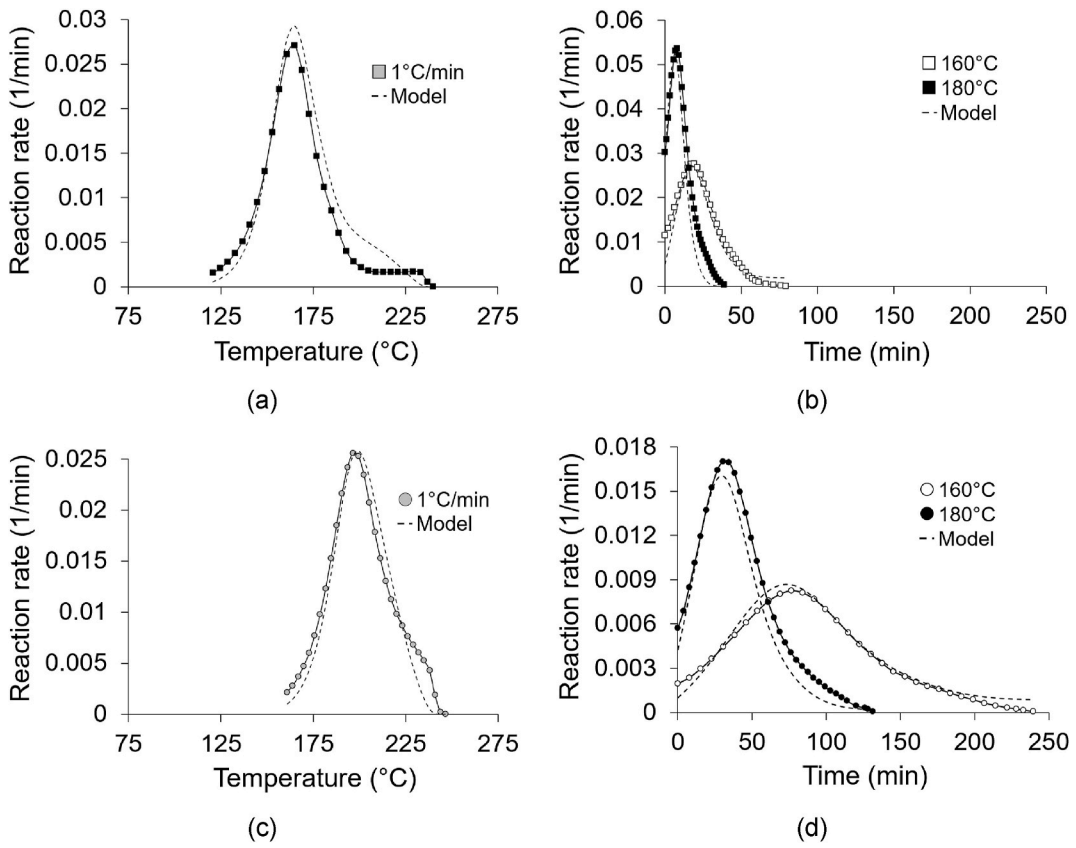

Fig. 2. Autocatalytic model fitting for the TGPAP/LNZ group: (a) dynamic and (b) isothermal data for the $E_1^{100}X_2^{100}$ binary blend; (c) dynamic and (d) isothermal data for the $E_1^{100}Y_2^{100}$ binary blend.

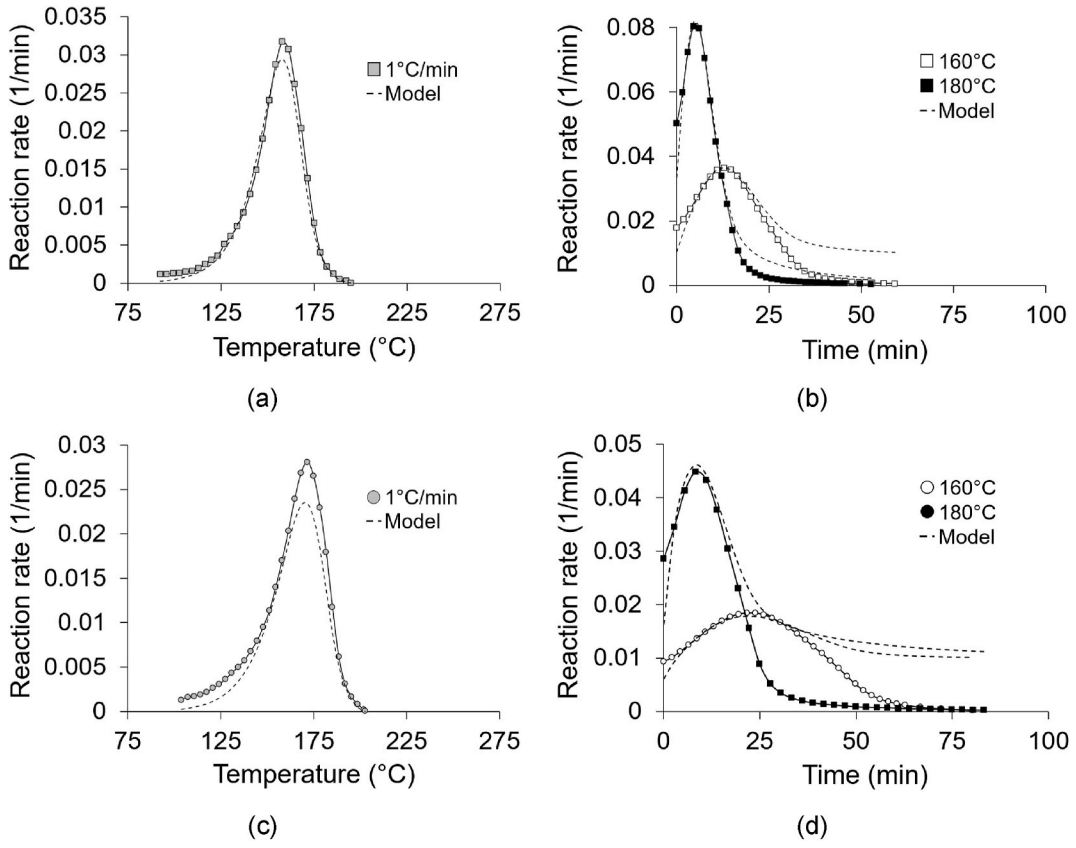

Fig. 3. Autocatalytic model fitting for the TGDDM/DDS group: (a) dynamic and (b) isothermal data for the $E_2^{100}X_1^{100}$ binary blend; (c) dynamic and (d) isothermal data for the $E_2^{100}Y_1^{100}$ binary blend.

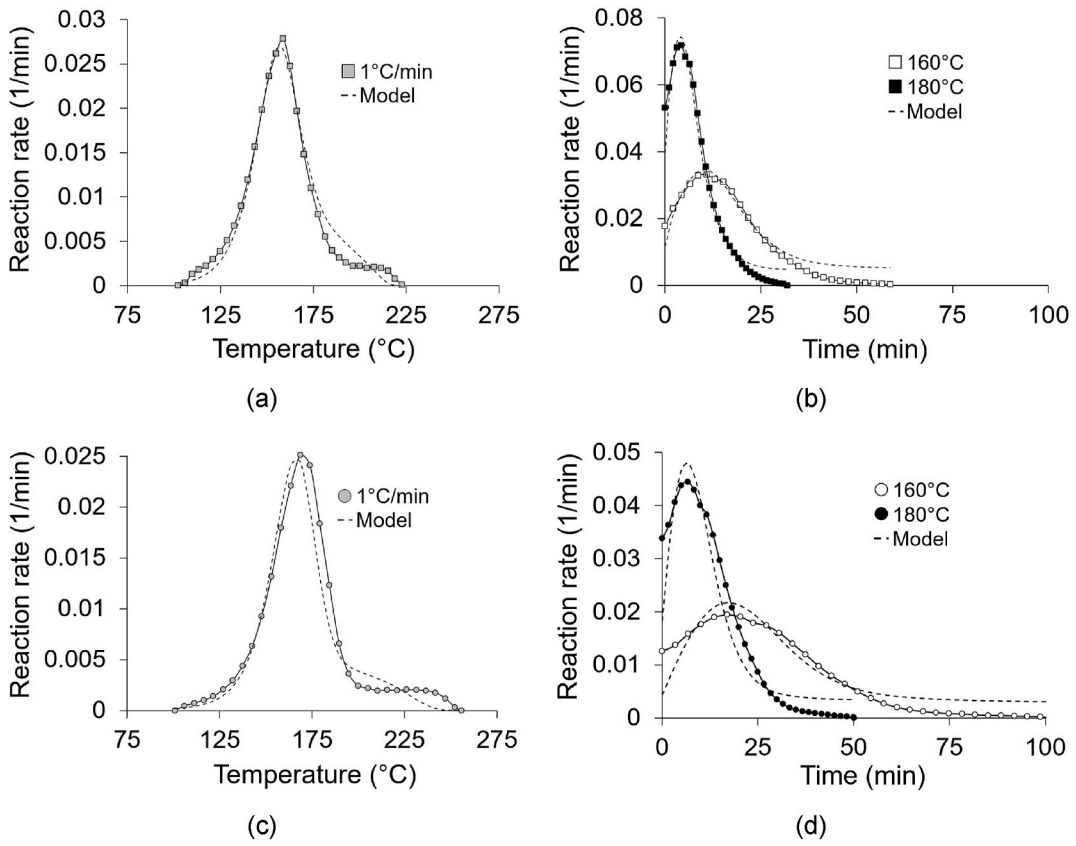

Fig. 4. Autocatalytic model fitting for the TGPAP/DDS/TP group: (a) dynamic and (b) isothermal data for the $E_1^{100}X_1^{100}$TP binary blend; (c) dynamic and (d) isothermal data for the $E_1^{100}Y_1^{100}$TP binary blend.

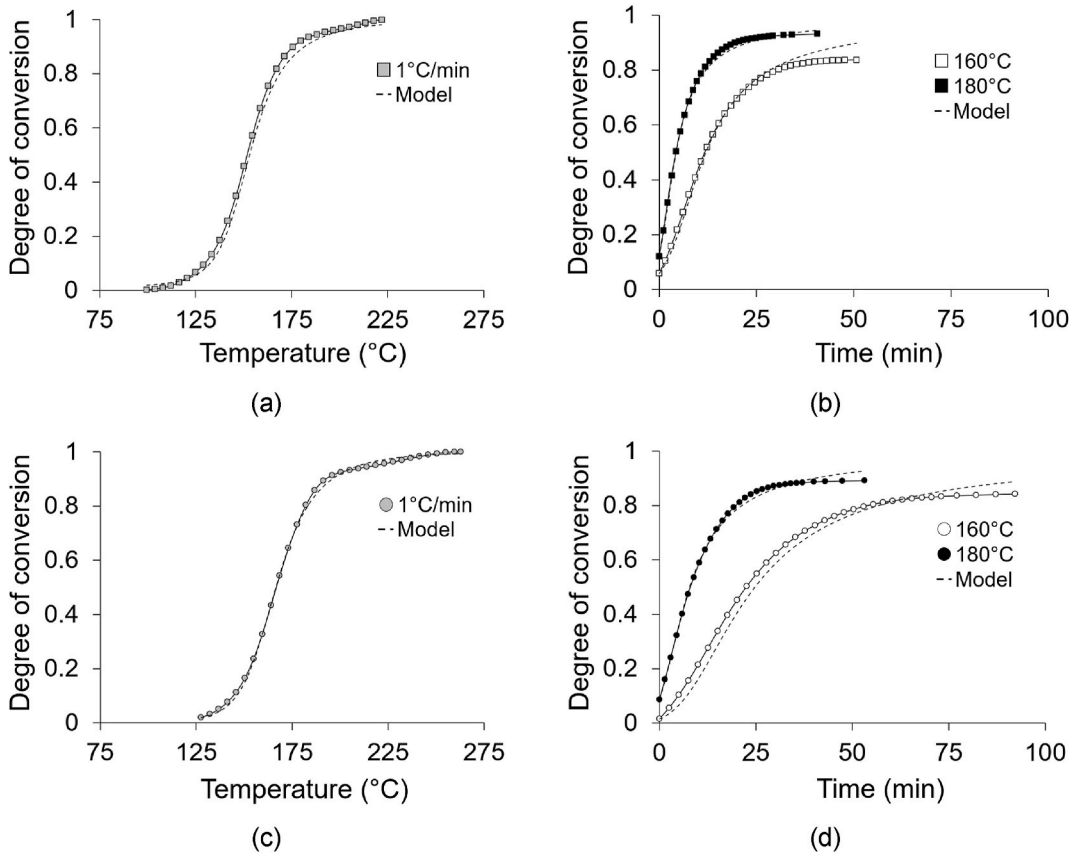

Fig. 5. Experimental and predicted conversion degree evolution of the TGPAP/DDS group: (a) dynamic and (b) isothermal data for the $E_1^{100}X_1^{100}$ binary blend; (c) dynamic and (d) isothermal data for the $E_1^{100}Y_1^{100}$ binary blend.

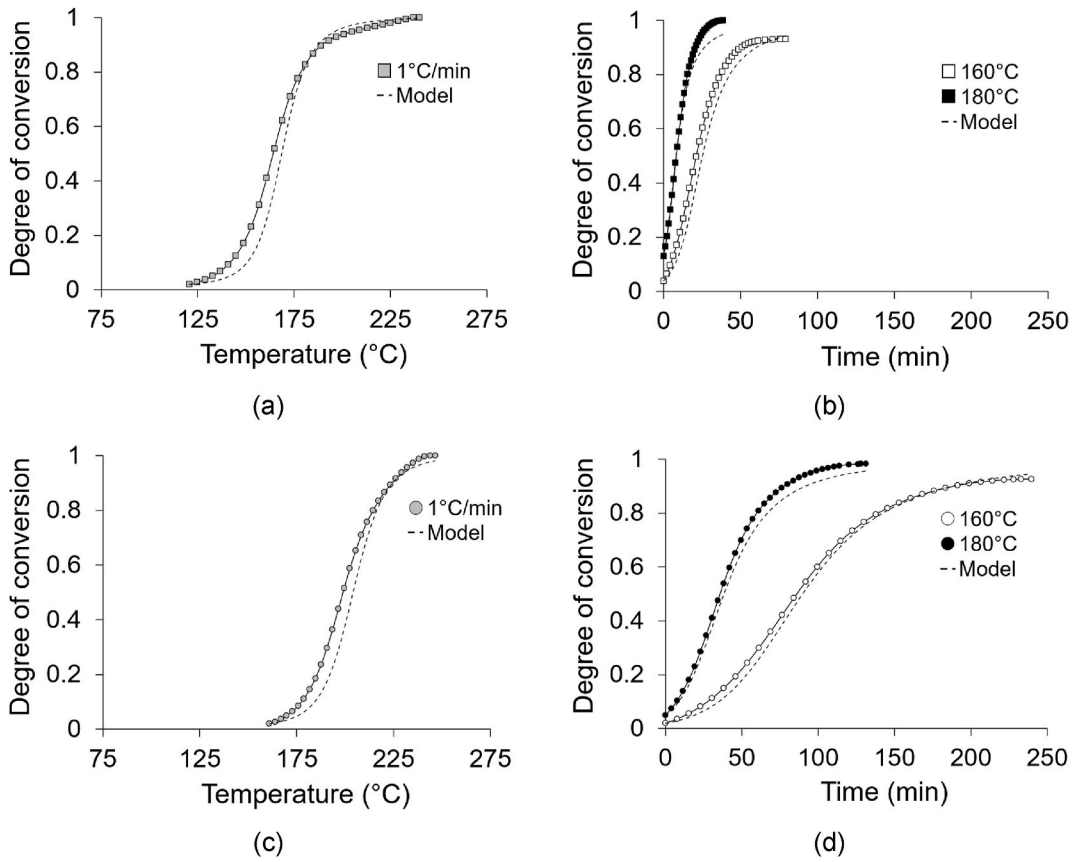

Fig. 6. Experimental and predicted conversion degree evolution of the TGPAP/LNZ group: (a) dynamic and (b) isothermal data for the $E_1^{100}X_2^{100}$ binary blend; (c) dynamic and (d) isothermal data for the $E_1^{100}Y_2^{100}$ binary blend.

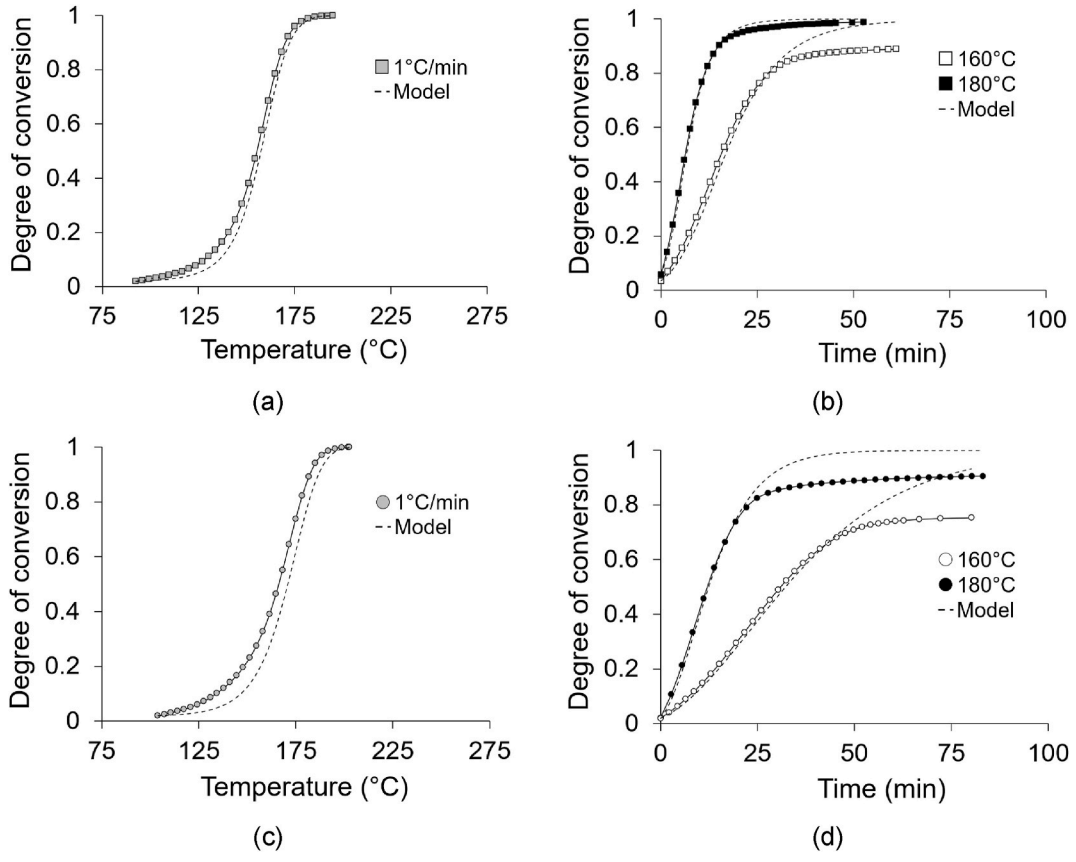

Fig. 7. Experimental and predicted conversion degree evolution of the TGDDM/DDS group: (a) dynamic and (b) isothermal data for the $E_2^{100}X_1^{100}$ binary blend; (c) dynamic and (d) isothermal data for the $E_2^{100}Y_1^{100}$ binary blend.

$$\left.\frac{d\alpha}{dt}\right|_{E_1E_2X} = f^{c}_{E_1} A_{E_1X} e^{-\frac{E_{E_1X}}{RT}} \alpha^{m_{E_1X}} (1-\alpha)^{n_{E_1X}} + f^{c}_{E_2} A_{E_2X} e^{-\frac{E_{E_2X}}{RT}} \alpha^{m_{E_2X}} (1-\alpha)^{n_{E_2X}} \quad (6)$$

where A_j is the pre-exponential factor, E_j the activation energy, and m_j, n_j the reaction orders of each binary blend with $j = (E_1X,\ E_2X)$.

The cure kinetics parameters of each binary blend (A_i, E_i, m_i, n_i, A_j, E_j, m_j, n_j) in Eqs. (4) and (6) were determined through application of the generalised reduced gradient non-linear optimisation method [61] to DSC results in order to minimise the error between prediction and experiment. Following this, the reaction rate of ternary blends can be determined in a predictive manner by changing the constituent functional group fractions (f_i^j) only. The initial degree of cure, which is required for use of an autocatalytic model, was set to 2%. This is necessary to allow to the model to start, as an initial value of zero would result in zero reaction rate in Eqs. (4) and (6). This assumption, which is necessary for the model to work mathematically, is also relevant to pre-cure taking place during resin preparation and mixing. As the extent of this initial reaction is unknown and cannot be determined accurately, the arbitrary value used becomes essentially a model parameter as the cure kinetics parameter values are associated with this assumption. Explicit integration was utilised to compute the evolution of the degree of cure with time.

Data underlying this study can be accessed through the Cranfield University repository at https://doi.org/10.17862/cranfield.rd.14500809 [dataset] [62].

3. Results and discussion

3.1. Cure kinetics of binary systems

Table 3 reports the cure kinetics parameters determined through curve fitting for all binary blends. The data for the MULTF/33DDS group are not listed as the kinetics data for $E_1^{100}X_1^{100}$, $E_2^{100}X_1^{100}$ binary blends can be inferred from the TGPAP/DDS and TGDDM/DDS groups respectively. The pre-exponential factor (A) is indicative of the molecular collision frequency and governs the width of the kinetics curve. The higher this value, the narrower the curve. The TGPAP/LNZ group achieves the lowest values in the 10^4-10^5 min^{-1} range, whilst the TGDDM/DDS group attains the highest values in the 10^7-10^8 min^{-1} range. The presence of thermoplastic in the TGPAP/DDS/TP matrix system reduces the pre-exponential factor by one order of magnitude versus the corresponding non-toughened TGPAP/DDS matrix set, which is indicative of a slower reaction in the toughened formulation in agreement with previous studies reporting a reduced reaction rate associated with dilution of the reactant species and mobility limitations [63–66]. The activation energy values (E_{ACT}) have the same order of 10^4 J/mol across all matrix sets. The TGPAP/LNZ matrix blends have the lowest values of activation energy than any other investigated group. The TGDDM/DDS group achieves higher values with the same curative as TGPAP/DDS, indicating that a higher temperature and greater molecular motion are required to initiate the reaction. The presence of thermoplastic causes very little effect on the activation energy suggesting that no relevant changes in the energy barrier required for initiation of the reaction occur compared to the corresponding non-toughened TGPAP/DDS system. The autocatalytic reaction order m, which ranges between 0.5 and 1.1, influences the curve position. The TGPAP/LNZ group has the highest m values as M-MIPA and M-CDEA are latent curing agents, whilst the TGDDM/DDS the lowest values. The reaction order n affects the curve amplitude and it varies in the range of 1.0–2.2. The TGDDM/DDS systems have the lowest n values.

Figs. 1–4 illustrate the results of the autocatalytic model fitting for the dynamic and isothermal experimental data generated for all binary blends; MULTF/33DDS is not explicitly reported as its binary blends

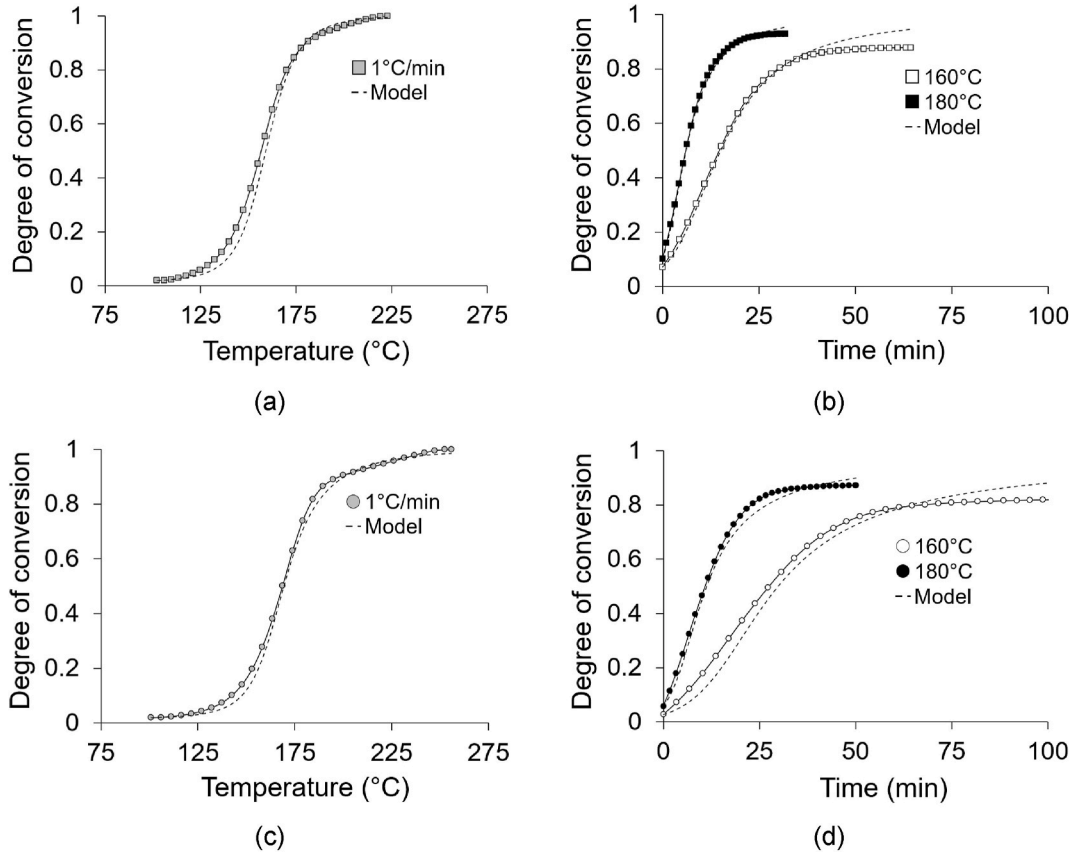

Fig. 8. Experimental and predicted conversion degree evolution of the TGPAP/DDS/TP group: (a) dynamic and (b) isothermal data for the $E_1^{100}X_1^{100}$TP binary blend; (c) dynamic and (d) isothermal data for the $E_1^{100}Y_1^{100}$TP binary blend.

($E_1^{100}X_1^{100}$, $E_2^{100}X_1^{100}$) can be deduced from the results of TGPAP/DDS and TGDDM/DDS. In all cases, the dynamic data are replicated with a satisfactory level of accuracy both in terms of amplitude and onset, peak and end reaction temperature. Small deviations towards the end of the reaction are observed for the TGPAP/DDS and TGPAP/LNZ matrix systems; these are associated with the onset of a secondary reaction mechanism which cannot be captured by a single-term autocatalytic model. The fitting of the isothermal data is adequate with some discrepancies after the main reaction peak due to the onset of diffusion phenomena which the kinetics model does not account for. The average absolute error in reaction rate between predicted and experimental values across the investigated binary blends is 0.001–0.005 min^{-1}.

The TGPAP/DDS matrix set is the most reactive system characterised by narrow curves and short cure times as shown in both dynamic and isothermal plots of Fig. 1. The $E_1^{100}X_1^{100}$ system containing 3,3′ DDS reacts at a lower temperature of about 100 °C versus 125 °C for $E_1^{100}Y_1^{100}$ which contains 4,4′ DDS, implying a slower reaction for the latter. The slower kinetics of the system containing 4,4′ DDS is also manifested in isothermal experiments in which cure is completed in longer times by about 50% compared to the system containing 3,3′ DDS. As observed in dynamic plots, both blends present a main reaction event followed by a secondary reaction at temperatures above 200 °C which is slightly more extended in the cure of the low-reactive binary blend.

The TGPAP/LNZ matrix set is characterised by a wide temperature reactivity window, as shown in Fig. 2. In the dynamic test, there is a 35 °C difference between the temperatures of the two maximum reaction peaks compared to a 10 °C difference for the corresponding case of the TGPAP/DDS group. In the dynamic experiments, the TGPAP/LNZ systems start reacting at higher temperatures with a steeper conversion rate gradient compared to the TGPAP/DDS due to this lower activation energy. In the isothermal tests, the TGPAP/LNZ cure curves span over longer cure times with broader reaction peaks compared to TGPAP/DDS. As the selected isothermal temperatures correspond to the initial reactivity stages of these materials, a longer exposure time is required for full conversion compared to TGPAP/DDS systems.

The TGDDM/DDS matrix set, illustrated in Fig. 3, differs in terms of pre-polymer functionality compared to the TGPAP/DDS set. However, its kinetics behaviour is similar to that of TGPAP/DDS as the matrix reactivity window is governed by the amine. The initial stages of the reaction are characterised by a lower conversion rate gradient which is manifested in the curve asymmetry between the ascending and descending phases of the reaction. The isothermal curing times are slightly longer, but still close to those of TGPAP/DDS.

The TGPAP/DDS/TP matrix set involves the presence of a thermoplastic modifier. As shown in Fig. 4, the autocatalytic model fitting of the toughened binary blends is satisfactory compared to the corresponding experimental results despite the expected deviation around the second reaction mechanism in the dynamic plots as the model is limited to a single autocatalytic behaviour. However, an unexpected slope change is observed after the main reaction peak in both isothermal curves which might be attributed to dissolution of the thermoplastic which interferes with the reaction evolution.

Figs. 5–8 compare the experimental and predicted degree of conversion for all the investigated binary systems across dynamic and isothermal profiles. The previous discussion about the reaction rate evolution confirms the observations on the degree of cure evolution strengthening the reliability and confidence in the performed reaction rate fitting. This returns an average difference on conversion degree between 1.6% and 5.6%. The predicted degree of conversion presents the minimum deviation from the experimental value in the $E_1^{100}X_1^{100}$, $E_1^{100}Y_1^{100}$ binary blends of the TGPAP/DDS group and in the $E_1^{100}X_1^{100}$TP, $E_1^{100}Y_1^{100}$TP binary blends of the TGPAP/DDS/TP group with an average

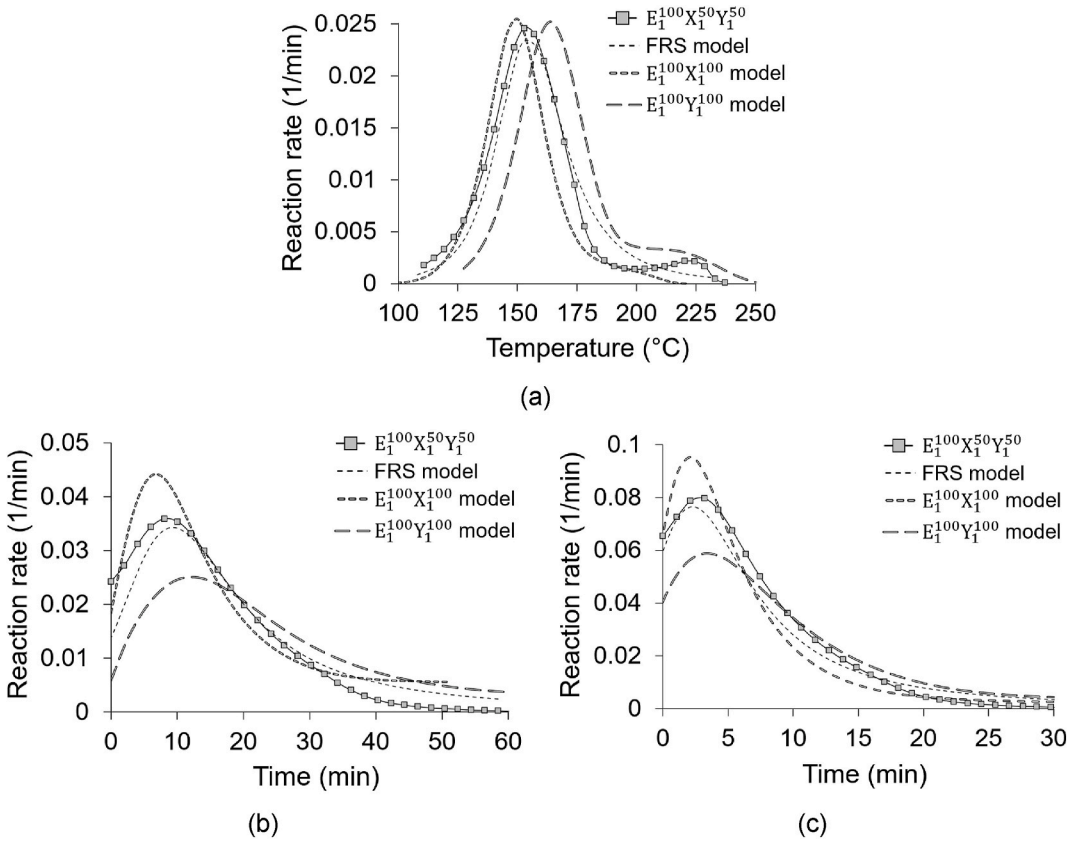

Fig. 9. Application of the FRS model to the $E_1^{100}X_1^{50}Y_1^{50}$ (TGPAP/DDS) ternary blend versus their corresponding experimental data set: (a) 1 °C/min heating rate profile, (b) 160 °C and (c) 180 °C temperature dwells.

conversion degree deviation for each set of 1.6% and 2.3% respectively, as shown in Figs. 5 and 8. In these cases, the prediction is very good as it follows closely the experimental trends with minimum deviations in line with the corresponding reaction rate fitting. As expected, the predicted degree of conversion diverges from the experimental value towards the end of the reaction in the isothermal plots due to the fact that diffusion effects are not included in the models. The $E_1^{100}X_2^{100}$, $E_1^{100}Y_2^{100}$ binary blends of the TGPAP/LNZ group and the $E_2^{100}X_1^{100}$, $E_2^{100}Y_1^{100}$ binary blends of the TGDDM/DDS group present greater differences in degree of conversion with an average conversion degree deviation for each set of 4.0% and 4.4% respectively, as shown in Figs. 6 and 7. In both cases, the model lags behind the experimental data in the chemically-controlled region, whilst the neglected diffusion effects result in a larger deviation at the later stages of the reaction mainly for the TGDDM/DDS matrix set which is mirrored in the corresponding reaction rate fitting. In any case, the maximum average error on conversion reaches 2.5% if the high conversion values around the diffusion region in the isothermal experiments are not taken into account.

3.2. Cure kinetics modelling of ternary systems

Figs. 9–13 illustrate the application of Formulation Ratio Superposition (FRS) to the ternary blends across all investigated groups in both dynamic and isothermal conditions. The experimentally determined evolution of the reaction of ternary blends is compared with the prediction of the models based on application of Eqs. (4) and (6) and the parameter values reported in Table 3 for the binary blends. The ternary blends with equally split constituent functional group fractions are reported only, as they represent the most distant cases from the limit cases of binary formulations. The experimental reaction rate for the ternary blends is intermediate to the predicted reaction rates of the binary materials. In all cases, the FRS model confirms this trend reproducing an autocatalytic reaction mechanism with an average reaction rate error of about 0.002 min^{-1}. Both predicted time/temperature and reaction rate of the ternary blend peaks are intermediate to the corresponding predicted values of the binary blends in all cases. The only exception is the dynamic data of the TGDDM/DDS ternary blend shown in Fig. 12(a). In this case the predicted temperature results are intermediate, but the reaction rate is higher than those of both binary materials by 0.001–0.007 min^{-1} respectively. However, this small difference can be attributed to potential variations of the baseline on which the fitting is based.

As illustrated in Figs. 9 and 10, the prediction is satisfactory for the TGPAP/DDS and the MULTF/33DDS matrix systems. The main deviations of the model from the experimental data, which are in the order of 0.003 min^{-1}, are attributed to the single autocatalytic process considered in the model, which neglects the minor secondary reaction mechanism above 200 °C observed in Fig. 9(a), and to the fact that diffusion-controlled phenomena, which can be observed in Fig. 9(b), (c) and Fig. 10(b), (c) arising towards the end of the reaction, are also not included in the kinetics model. Table 4 indicates the maximum degree of conversion determined in isothermal temperature profiles for the ternary blends and compares them with the predicted values. The model predicts conversion degrees greater or equal to the experimental data as it does not take into account diffusion phenomena. These findings support the validity of the approach in predicting the cure behaviour either of a one epoxy/two amines system or two epoxies/one amine system.

Similar observations apply to the TGPAP/LNZ and TGDDM/DDS systems reported in Figs. 11 and 12. The model discrepancies are exacerbated in the TGPAP/LNZ dynamic cure experiment of Fig. 11(a) with the predicted reaction rate peak being higher by about 0.008 min^{-1} than in the experiment and the predicted curve narrower as the energy content associated to the second reaction mechanism of the experiment

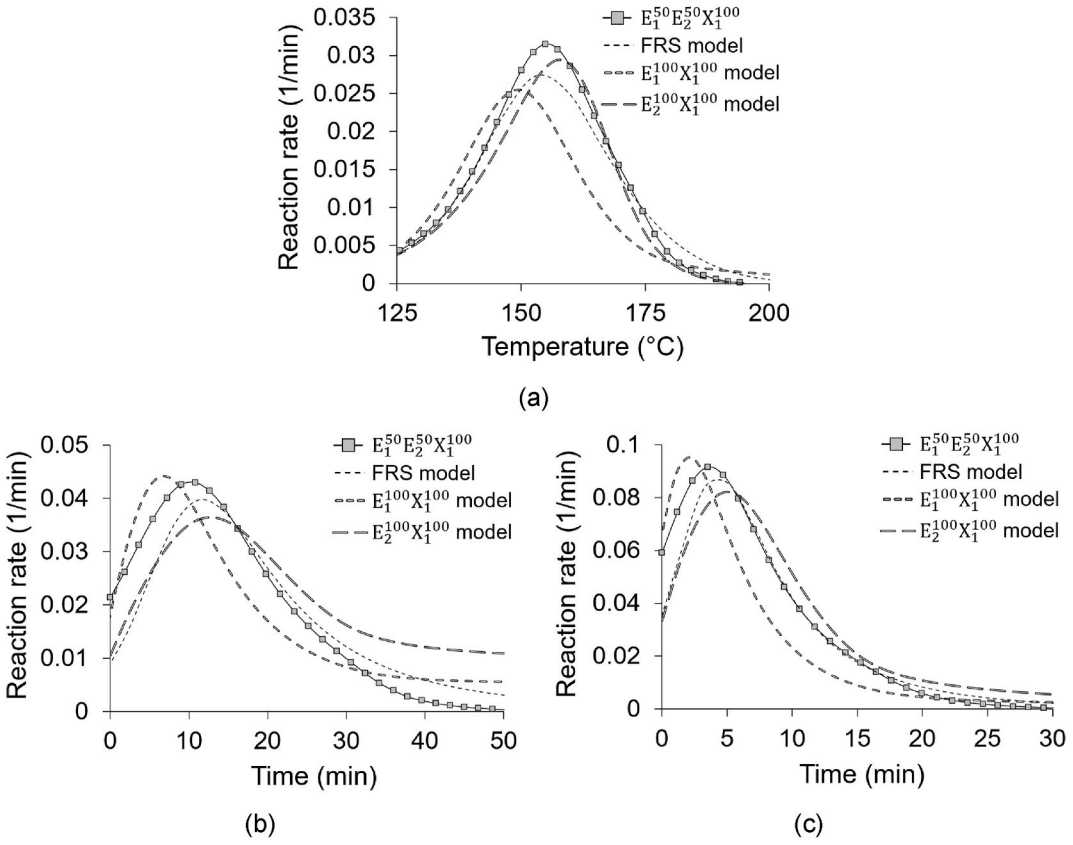

Fig. 10. Application of the FRS model to the $E_1^{50}E_2^{50}X_1^{100}$ (MULTF/33DDS) ternary blend versus their corresponding experimental data set: (a) 1 °C/min heating rate profile, (b) 160 °C and (c) 180 °C temperature dwells.

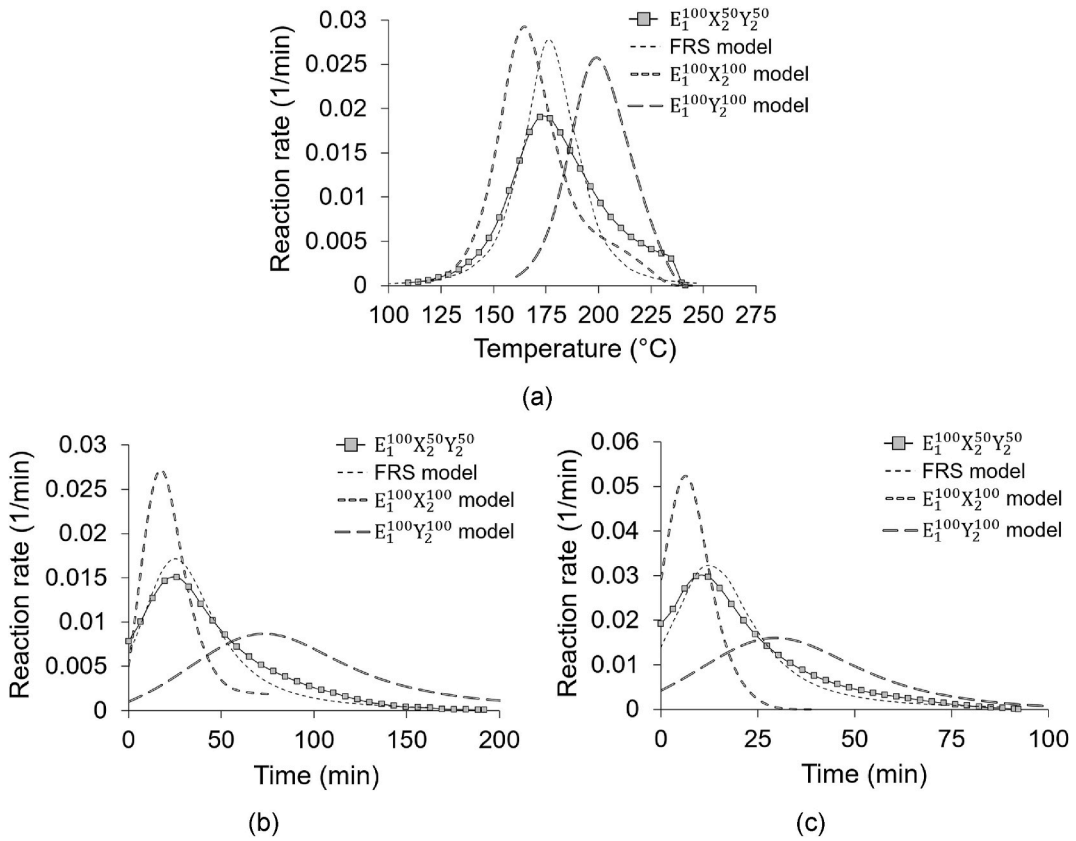

Fig. 11. Application of the FRS model to the $E_1^{100}X_2^{50}Y_2^{50}$ (TGPAP/LNZ) ternary blend versus their corresponding experimental data set: (a) 1 °C/min heating rate profile, (b) 160 °C and (c) 180 °C temperature dwells.

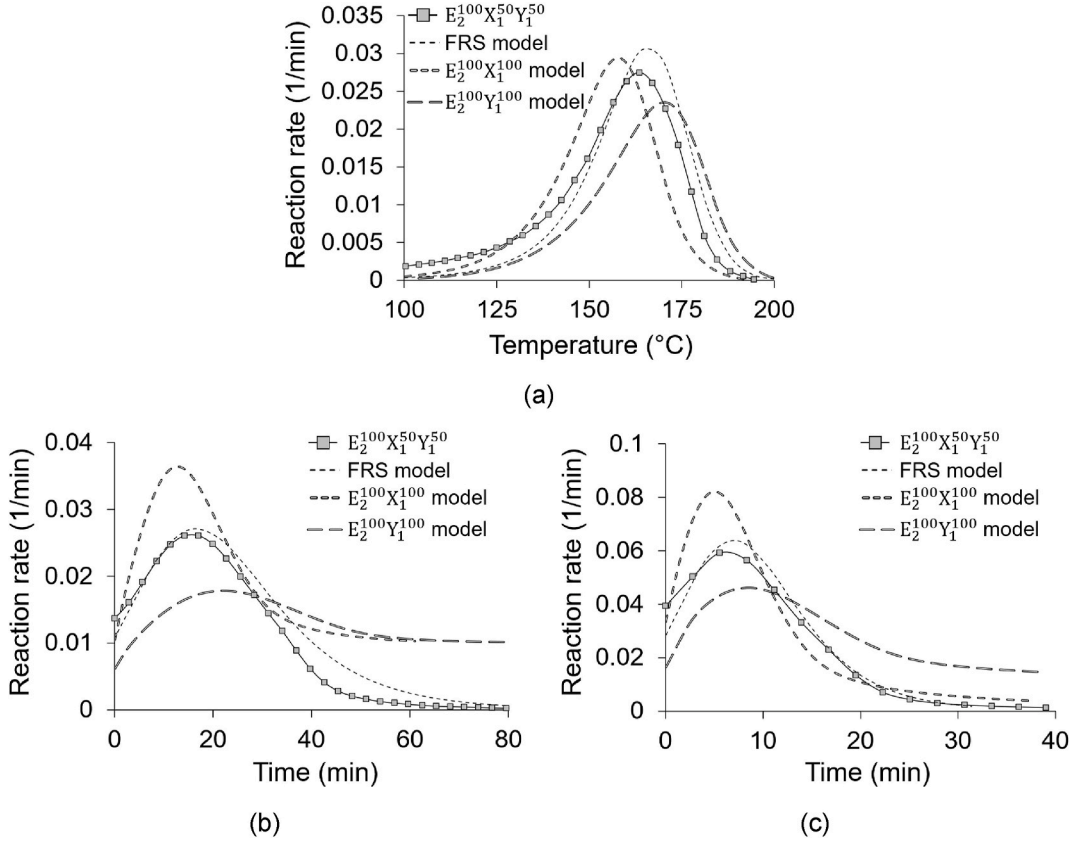

Fig. 12. Application of the FRS model to the $E_2^{100}X_1^{50}Y_1^{50}$ (TGDDM/DDS) ternary blend versus their corresponding experimental data set: (a) 1 °C/min heating rate profile, (b) 160 °C and (c) 180 °C temperature dwells.

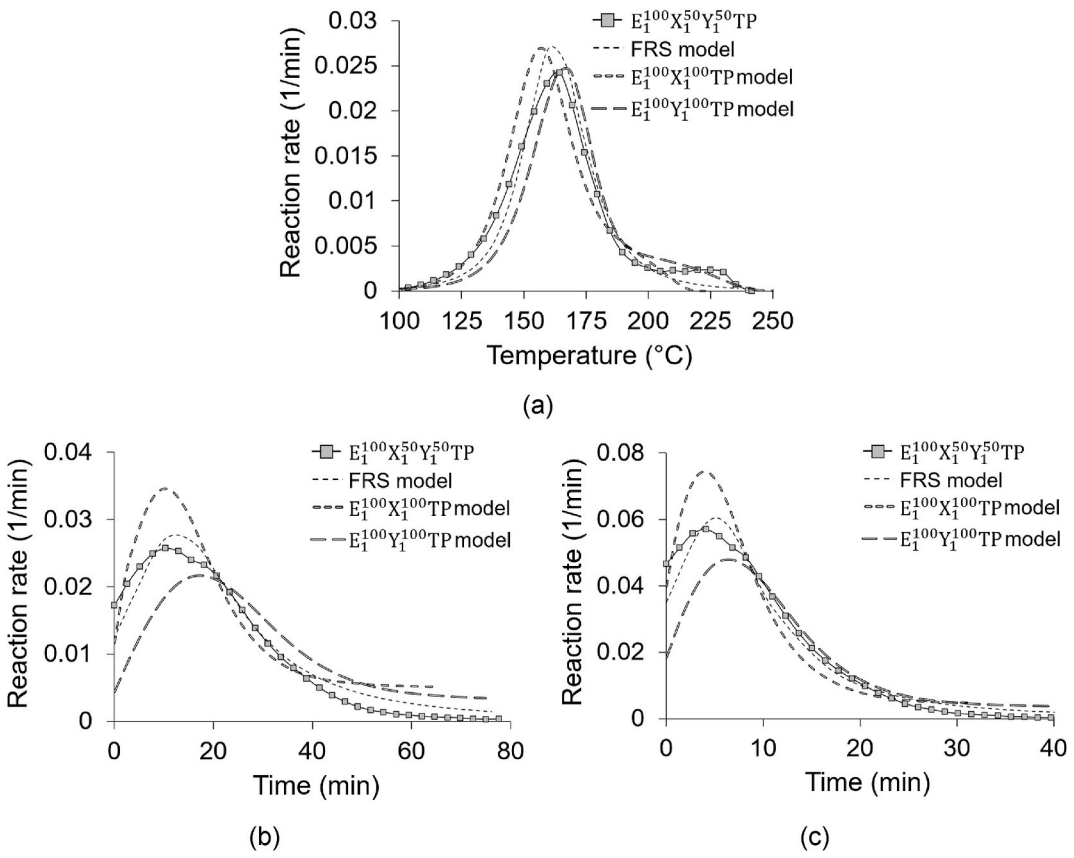

Fig. 13. Application of the FRS model to the $E_1^{100}X_1^{50}Y_1^{50}TP$ (TGPAP/DDS/TP) ternary blend versus their corresponding experimental data set: (a) 1 °C/min heating rate profile, (b) 160 °C and (c) 180 °C temperature dwells.

Table 4
Comparison on experimental and predicted maximum conversion degrees achieved in isothermal cure conditions for ternary systems.

Group	Matrix	Degree of conversion at 160 °C dwell		Degree of conversion at 180 °C dwell	
		Predicted	Experimental	Predicted	Experimental
TGPAP/DDS	$E_1^{100}X_1^{50}Y_1^{50}$	0.89	0.83	0.91	0.89
	$E_1^{100}X_1^{20}Y_1^{80}$	0.91	0.82	0.92	0.88
	$E_1^{100}X_1^{40}Y_1^{60}$	0.88	0.82	0.93	0.89
	$E_1^{100}X_1^{70}Y_1^{30}$	0.91	0.82	0.93	0.88
	$E_1^{100}X_1^{90}Y_1^{10}$	0.92	0.82	0.95	0.89
MULTF/33DDS	$E_1^{50}E_2^{50}X_1^{100}$	0.95	0.95	0.98	0.98
TGPAP/LNZ	$E_1^{100}X_2^{50}Y_2^{50}$	0.98	0.96	0.98	0.98
	$E_1^{100}X_2^{20}Y_2^{80}$	0.97	0.91	0.98	0.98
	$E_1^{100}X_2^{40}Y_2^{60}$	0.97	0.94	0.98	0.98
	$E_1^{100}X_2^{70}Y_2^{30}$	0.97	0.94	0.98	0.98
	$E_1^{100}X_2^{90}Y_2^{10}$	0.95	0.92	0.99	0.99
TGDDM/DDS	$E_2^{100}X_1^{50}Y_1^{50}$	0.99	0.83	0.99	0.95
	$E_2^{100}X_1^{20}Y_1^{80}$	0.98	0.78	0.99	0.92
	$E_2^{100}X_1^{40}Y_1^{60}$	0.98	0.82	0.99	0.94
	$E_2^{100}X_1^{70}Y_1^{30}$	0.99	0.86	0.99	0.96
	$E_2^{100}X_1^{90}Y_1^{10}$	0.99	0.87	0.99	0.99
TGPAP/DDS/TP	$E_1^{100}X_1^{50}Y_1^{50}TP$	0.93	0.84	0.94	0.89

is included in the single mechanism considered in the model. As the reaction rate is proportional to the heat flow and the reaction energy content must be the same as the one of the experiment, the model tends to shrink the curve in the temperature direction and stretch it in the reaction rate direction so that the area under the curve is representative of full cure. The difference between experimental and predicted ternary blend peak reaction is lower in the isothermal data shown in Fig. 11(b) and (c) as the phenomenon is compensated by greater reaction towards

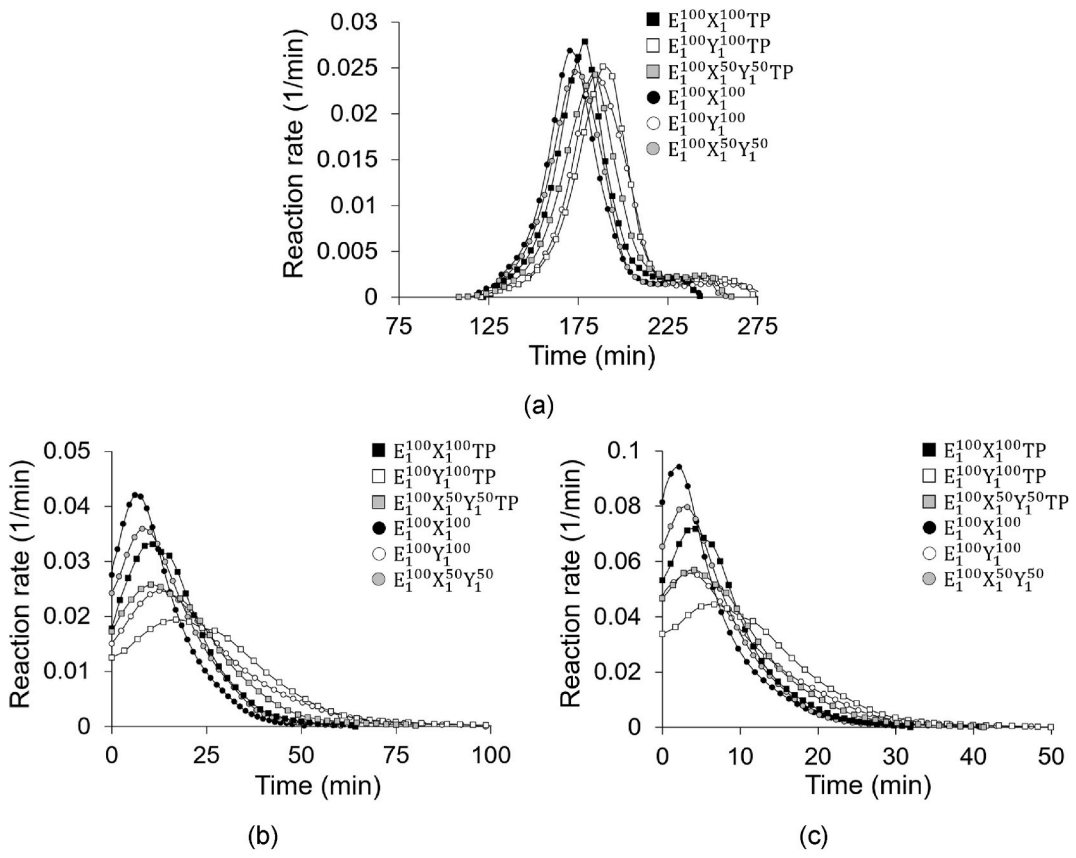

Fig. 14. Reaction rate comparison between TGPAP/DDS and TGPAP/DDS/TP matrix systems on the $E_1^{100}X_1^{50}Y_1^{50}TP$ (TGPAP/DDS/TP) ternary blend versus their corresponding experimental data set: (a) 1 °C/min heating rate profile, (b) 160 °C and (c) 180 °C temperature dwells.

the end of the cure in the model. The average reaction rate error measured across both dynamic and isothermal data is about 0.003 min^{-1}. Similarly, the correspondence between model and experiment in the TGDDM/DDS group is acceptable with an average reaction rate error of 0.002 min^{-1}. In the dynamic plot of Fig. 12(a), the difference in peak heights is affected by baseline variations, whilst in the isothermal plots of Fig. 12(b) and (c) the deviation towards the end of the reaction of both binary blend models is linked to the fitting of the model which does not consider diffusion effects leading to a non-zero reaction rate plateau. These findings extend the applicability of the FRS model also to matrix systems with a wide curative reactivity range and to matrix systems with higher functionality.

Table 5
Average reaction rate error of the FRS model for the ternary blends.

Matrix blend	Ternary blend	Average reaction rate error (min^{-1})
TGPAP/DDS	$E_1^{100}X_1^{20}Y_1^{80}$	0.0018
	$E_1^{100}X_1^{40}Y_1^{60}$	0.0019
	$E_1^{100}X_1^{50}Y_1^{50}$	0.0025
	$E_1^{100}X_1^{70}Y_1^{30}$	0.0018
	$E_1^{100}X_1^{90}Y_1^{10}$	0.0015
MULTF/33DDS	$E_1^{50}E_2^{50}X_1^{100}$	0.0028
TGPAP/LNZ	$E_1^{100}X_2^{20}Y_2^{80}$	0.0018
	$E_1^{100}X_2^{40}Y_2^{60}$	0.0021
	$E_1^{100}X_2^{50}Y_2^{50}$	0.0031
	$E_1^{100}X_2^{70}Y_2^{30}$	0.0018
	$E_1^{100}X_2^{90}Y_2^{10}$	0.0018
TGDDM/DDS	$E_2^{100}X_1^{20}Y_1^{80}$	0.0020
	$E_2^{100}X_1^{40}Y_1^{60}$	0.0020
	$E_2^{100}X_1^{50}Y_1^{50}$	0.0017
	$E_2^{100}X_1^{70}Y_1^{30}$	0.0015
	$E_2^{100}X_1^{90}Y_1^{10}$	0.0013
TGPAP/DDS/TP	$E_1^{100}X_1^{50}Y_1^{50}TP$	0.0020

Fig. 13 reports the results for the TGPAP/DDS/TP group for both dynamic and isothermal data which confirm the intermediate kinetics behaviour of the ternary blend. The FRS holds even in this scenario showing a satisfactory match to the experimental data both in terms of curve width and maximum reaction peak value. Although the toughener does not contribute to the cure, it slows down the reaction progress as demonstrated in the reaction rate curves of Fig. 14 which compares the toughened system to the non-toughened TGPAP/DDS matrix set under dynamic and isothermal data. All toughened systems are shifted towards the right along the time axis; however, they still maintain the relative positions among binary and ternary blends. With equal masses for the toughened and non-toughened matrix blends, the addition of a modifier component reduces the mass of both the epoxy and the curing agent. This results in a lower probability that epoxides and amine active hydrogen groups crosslink and therefore in a reduced reaction rate. This effect has been observed in similar matrix systems for different percentages of tougheners and for similar matrix system constituents [63–66].

Table 5 summarises the average reaction rate absolute error for all investigated blends which falls within the 0.001–0.003 min^{-1} interval. The maximum error of 0.0031 min^{-1} occurs in the $E_1^{100}X_2^{50}Y_2^{50}$ (TGPAP/LNZ) blend, whilst the minimum value of 0.0013 min^{-1} in the $E_2^{100}X_1^{90}Y_1^{10}$ (TGDDM/DDS) blend. This error range can be considered satisfactory as it is one order of magnitude lower than the determined reaction rate values; as a general trend, the deviation tends to be

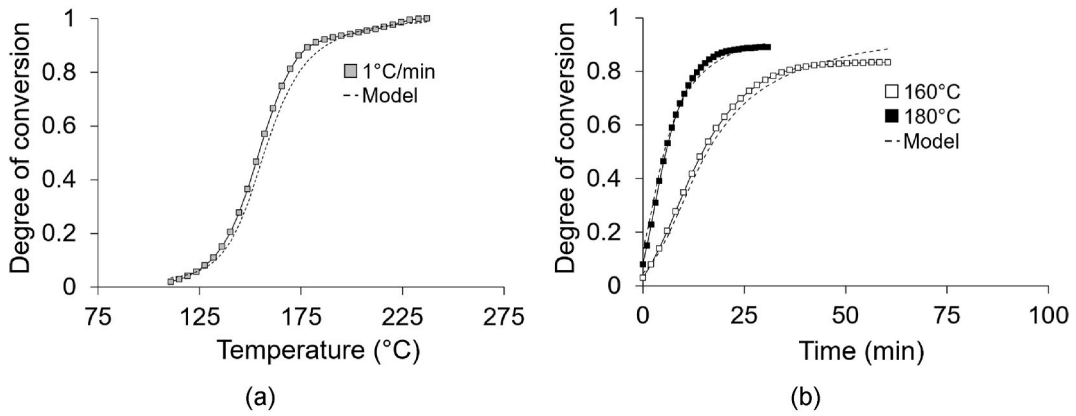

Fig. 15. Experimental and predicted conversion degree evolution of the $E_1^{100}X_1^{50}Y_1^{50}$ (TGPAP/DDS) ternary blend: (a) dynamic and (b) isothermal data.

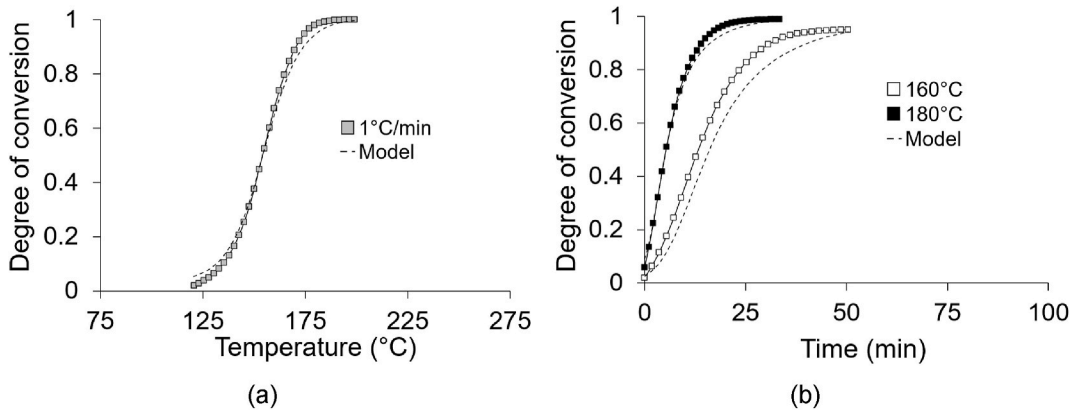

Fig. 16. Experimental and predicted conversion degree evolution of the $E_1^{50}E_2^{50}X_1^{100}$ (MULTF/33DDS) ternary blend: (a) dynamic and (b) isothermal data.

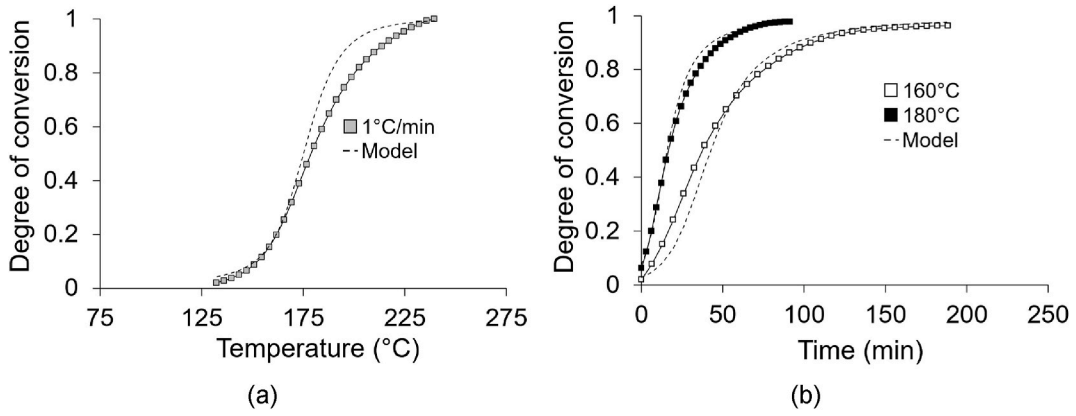

Fig. 17. Experimental and predicted conversion degree evolution of the $E_1^{100}X_2^{50}Y_2^{50}$ (TGPAP/LNZ) ternary blend: (a) dynamic and (b) isothermal data.

minimal in the chemically controlled reaction stages, whilst it is enhanced by the onset of diffusion phenomena which have not been taken into the model. These findings confirm the reliability of the FRS model to predict any intermediate reaction behaviour for ternary matrix systems starting from constitutive models of the binary materials.

Figs. 15–19 compare the predicted degree of cure to the calorimetry data for all the investigated ternary systems with equal distribution of constituent fractional groups. The prediction is satisfactory in the chemically-controlled region, whilst it tends to deviate from the experiment when diffusion starts playing a dominant role towards the end of the reaction under isothermal conditions. The average error in degree of conversion ranges between 2.6% and 6.4% for the TGPAP/DDS and TGDDM/DDS matrix sets respectively. The major deviations resulting in the $E_1^{100}X_2^{50}Y_2^{50}$ blend of the TGPAP/LNZ group and in the $E_2^{100}X_1^{50}Y_1^{50}$ blend of the TGDDM/DDS group, as shown in Figs. 17 and 18 respectively, mirror the fitting of the binary systems kinetics for these sets with an average error in degree of conversion of 3.9% and 6.4% respectively. This is also evident in the $E_1^{50}E_2^{50}X_1^{100}$ blend of the MULTF/33DDS matrix set shown in Fig. 16 where the weighted contribution from the $E_2^{100}X_1^{100}$ binary blend of the TGDDM/DDS group influences the trend in the isothermal profiles which results in a 3.5% average error. Compared to the TGPAP/DDS group, the addition of a thermoplastic component in the TGPAP/DDS/TP group results in a milder evolution of the cure. As

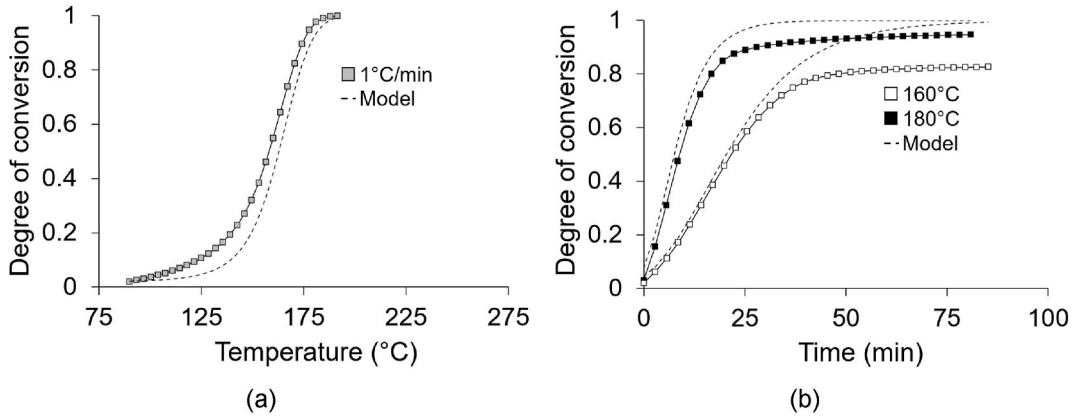

Fig. 18. Experimental and predicted conversion degree evolution of the $E_2^{100}X_1^{50}Y_1^{50}$ (TGDDM/DDS) ternary blend: (a) dynamic and (b) isothermal data.

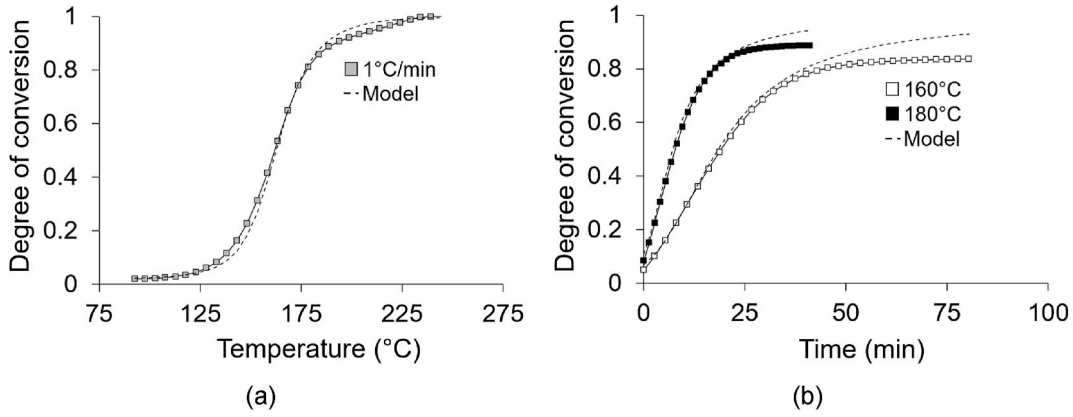

Fig. 19. Experimental and predicted conversion degree evolution of the $E_1^{100}X_1^{50}Y_1^{50}$TP (TGPAP/DDS/TP) ternary blend: (a) dynamic and (b) isothermal data.

shown in Fig. 15 for the $E_1^{100}X_1^{50}Y_1^{50}$ blend of the TGPAP/DDS set and in Fig. 19 for the $E_1^{100}X_1^{50}Y_1^{50}$TP of the TGPAP/DDS/TP set, the prediction reproduces the experimental progress of the cure successfully. In both cases, the average deviation on degree of conversion is around 2.6%.

The results presented demonstrate that the FRS methodology provides a valid approximation and can be used as part of the formulation process. This approach overcomes the complexity associated with mechanistic modelling, whilst further enhancing kinetics phenomenological modelling by introducing an explicit connection to matrix composition. The proposed methodology allows to adjust the cure reaction characteristics of a ternary formulation focusing on a weighted superposition of the reaction rates of its individual-pair constituents. Reactivity and time-to-react of complex matrix formulations can be tailored in an automated fashion tuning the constituent fractions of individual epoxy/amine blends with different molecular weights and reactivities. The FRS methodology can be applied to any type of phenomenological cure model incorporating more mechanisms and diffusion control terms. Furthermore, the FRS approach has the potential to be extended to non-epoxy formulations.

4. Conclusions

The proposed cure kinetics methodology establishes an explicit connection between material chemistry and material modelling overcoming traditional limitations of standard cure kinetics phenomenological techniques and reducing experimental effort and development time for resin formulation. The Formulation Ratio Superposition (FRS) approach has been demonstrated to approximate satisfactorily the kinetics of ternary blends over a wide variety of amine/epoxy systems. Matrix formulations can be tailored to specific design requirements controlling reaction intensity and time-to-react by changing the constituent functional group fraction. The characterisation of the binary blend cure kinetics and the parameterisation of the matrix constituent functional groups provide greater design flexibility, as complex matrix formulations can be tailored to improve toughness, damage tolerance and environmental stability. This cure kinetics modelling strategy could also be extended to matrix systems with more than three constituents and potentially support the development of bespoke raw chemicals with an intermediate behaviour. The FRS approach is also potentially useful to manage matrix exothermic risk by adapting the formulation to specific composite laminate thicknesses and spanning the reaction progress across a convenient temperature range. In this perspective, the FRS model can be integrated in a thermal cure process simulation and component cure optimisation algorithm to identify efficient matrix formulations suitable for high-rate cure cycles that minimise potential process failures due to temperature overshoots.

Dataset

Data underlying this study can be accessed through the Cranfield University repository at https://doi.org/10.17862/cranfield.rd.14500809 [dataset] [62].

CRediT authorship contribution statement

Gabriele Voto: Conceptualization, Methodology, Validation, Formal analysis, Investigation, Data curation, Writing – original draft, Visualization, Project administration. **Leela Sequeira:** Resources, Writing – review & editing, Supervision, Project administration. **Alexandros A.**

Skordos: Conceptualization, Methodology, Resources, Writing – review & editing, Supervision, Project administration, Funding acquisition.

Declaration of competing interest

The authors declare that they have no known competing financial interests or personal relationships that could have appeared to influence the work reported in this paper.

Acknowledgements

This work was supported by the Engineering and Physical Sciences Research Council through the EPSRC Centre for Doctoral Training in Composites Manufacture [grant number EP/K50323X/1].

References

[1] C.A. May, Resins for aerospace, J. Appl. Polym. Sci. (1985) 557–580. ACS Symposium Series 285.
[2] F.-L. Jin, X. Li, S.-J. Park, Synthesis and applications of epoxy resins: a review, J. Ind. Eng. Chem. 29 (2015) 1–11.
[3] M.A. Boyle, C.J. Martin, J.D. Neuner, Epoxy resins, in: ASM Handbook Volume 21 Composites, ASM International, Materials Park, 2001, pp. 78–89.
[4] W.R. Ashcroft, Curing agents for epoxy resins, in: Chemistry and Technology of Epoxy Resins, Springer, Dordrecht, 1993, pp. 37–71.
[5] H.S. Chu, J.C. Seferis, Network structure description and analysis of amine-cured epoxy matrices, in: The Role of the Polymeric Matrix in the Processing and Structural Properties Composite Materials, Springer, 1983, pp. 53–125.
[6] M. Holmes, Aerospace looks to composites for solutions, Reinforc Plast 61 (4) (2017) 237–241.
[7] Aerospace Technology Institute. UK aerospace technology strategy: aerostructures roadmap. Available at: https://www.ati.org.uk/media/qyonqp0v/aerostructures.pdf (Accessed: 10 02 2020).
[8] Aerospace Technology Institute. Aerospace composite technology roadmapping. Available at: https://compositesuk.co.uk/system/files/ATI%20Composite%20Roadmapping%20Results%202019.pdf (Accessed: 10 02 2020).
[9] Z.-S. Guo, S.-Y. Du, B. Zhang, Z. Wu, Cure characterization of a new bismaleimide resin using differential scanning calorimetry, J. Macromol. Sci. A 43 (11) (2006) 1687–1693.
[10] J.M. Kenny, G. Pisaniello, F. Farina, S. Puzziello, Calorimetric analysis of the polymerization reaction of a phenolic resin, Thermochim. Acta 269–270 (C) (1995) 201–211.
[11] D. Dean, M.A. Abdalla, U. Vaidya, R. Ganguli, C.J. Battle, A. Abdalla, A. Haque, S. Campbell, Processable PMR-type polyimides: process-property relationships, curing kinetics and thermooxidative stability, High Perform. Polym. 17 (4) (2005) 497–514.
[12] R.B. Prime, E. Sacher, Kinetics of epoxy cure: 2. The system bisphenol-A diglycidyl ether/polyamide, Polymer 13 (9) (1972) 455–458.
[13] R.B. Prime, Differential scanning calorimetry of the epoxy cure reaction, Polym. Eng. Sci. 13 (5) (1973) 365–371.
[14] J.M. Kenny, A. Trivisano, Isothermal and dynamic reaction kinetics of high performance epoxy matrices, Polym. Eng. Sci. 31 (19) (1991) 1426–1433.
[15] J.M. Kenny, A. Trivisano, M.E. Frigione, L. Nicolais, Thermal analysis of standard and toughened high-performance epoxy matrices, Thermochim. Acta 1999 (C) (1992) 213–227.
[16] M.R. Keenan, Autocatalytic cure kinetics from DSC measurements: zero initial cure rate, J. Appl. Polym. Sci. 33 (5) (1987) 1725–1734.
[17] S. Du, Z.-S. Guo, B. Zhang, Z. Wu, Cure kinetics of an epoxy resin used for advanced composites, Polym. Int. 53 (9) (2000) 1343–1347.
[18] M.R. Kamal, S. Sourour, Kinetics and thermal characterization of thermoset cure, Polym. Eng. Sci. 13 (1) (1973) 59–64.
[19] T.A. Bogetti, J.W. Gillespie Jr., Process-induced stress and deformation in thick-section thermoset composite laminates, J. Compos. Mater. 26 (5) (1992) 626–660.
[20] P.W.K. Lam, H.P. Plaumann, T. Tran, An improved kinetic model for the autocatalytic curing of styrene-based thermoset resins, J. Appl. Sci. 41 (11–12) (1990) 3043–3357.
[21] J.H. Lee, J.W. Lee, Kinetic parameters estimation for cure reaction of epoxy based vinyl ester resin, Polym. Eng. Sci. 34 (9) (1994) 742–749.
[22] M.R. Kamal, Thermoset characterization for moldability analysis, Polym. Eng. Sci. 14 (3) (1974) 231–239.
[23] M.R. Kamal, M.E. Ryan, The behaviour of thermosetting compounds in injection molding cavities, Polym. Eng. Sci. 20 (13) (1980) 859–867.
[24] J. Mijović, J. Kim, J. Slaby, Cure kinetics of epoxy formulations of the type used in advanced composites, J. Appl. Polym. Sci. 29 (4) (1984) 1449–1462.
[25] W.I. Lee, A.C. Loos, G.S. Springer, Heat of reaction, degree of cure and viscosity of Hercules 3501-6 resin, J. Compos. Mater. 16 (6) (1982) 509–520.
[26] J.M. Kenny, Determination of autocatalytic kinetic model parameters describing thermoset cure, J. Appl. Polym. Sci. 51 (4) (1994) 761–764.
[27] E.P. Scott, Z. Saad, Estimation of kinetic parameters associated with the curing of thermoset resins. Part II: experimental results, Polym. Eng. Sci. 33 (18) (1993) 1165–1169.
[28] M.A. Stone, B.K. Fink, T.A. Bogetti, J.W. Gillespie Jr., Thermo-chemical response of vinyl-ester resin, Polym. Eng. Sci. 40 (12) (2000) 2489–2497.
[29] L. Zemni, G. Dusserre, G. Bernhart, B. Boniface, A study of cross-linking kinetics of cyanate ester resin, in: Proceedings of 21st International Conference on Composite Materials (ICCM-21). Xi'an, August, 2016.
[30] P.I. Karkanas, I.K.P. Partridge, Modelling the cure of a commercial epoxy resin for applications in resin transfer moulding, Polym. Int. 41 (2) (1996) 183–191.
[31] P.I. Karkanas, I.K.P. Partridge, Cure modeling and monitoring of the epoxy/amine resin system. I. Cure kinetics modeling, J. Appl. Polym. Sci. 77 (7) (2000) 1419–1431.
[32] T. Mesogitis, J. Kratz, A.A. Skordos, Heat transfer simulation of the cure of thermoplastic particle interleaf carbon fibre epoxy prepregs, J. Compos. Mater. 53 (15) (2019) 2053–2064.
[33] J. Kratz, T. Mesogitis, A.A. Skordos, I. Hamerton, I.K.P. Partridge, Developing cure kinetics models for interleaf particle toughened epoxies, in: Proceedings of the International SAMPE Technical Conference, Long Beach, May 2016.
[34] G. Struzziero, B. Remi, A.A. Skordos, Measurement of thermal conductivity of epoxy resins during cure, J. Appl. Polym. Sci. 136 (5) (2019).
[35] S.-N. Lee, M.-T. Chiu, H.-S. Lin, Kinetic model for the curing reaction of a tetraglycidyl diamino diphenyl methane/diamino diphenyl sulfone (TGDDM/DDS) epoxy resin system, Polym. Eng. Sci. 32 (15) (1992) 10237–11046.
[36] A.A. Johnston, An Integrated Model of the Development of Process-Induced Deformation in Autoclave Processing of Composite Structures. PhD Thesis, The University of British Columbia, 1997.
[37] P. Hubert, A.A. Johnston, A. Poursartip, K. Nelson, Cure kinetics and viscosity model for Hexcel 8552 epoxy resin, in: Proceedings of International SAMPE Symposium and Exhibition, Long Beach, May 2001.
[38] L. Khoun, T. Centea, P. Hubert, Characterization methodology of thermoset resins for the processing of composite materials – case study: CYCOM 890RTM epoxy resin, J. Compos. Mater. 44 (11) (2010) 1397–1415.
[39] A. Dimopoulos, A.A. Skordos, I.K.P. Partridge, Cure kinetics, glass transition temperature development and dielectric spectroscopy of a low temperature cure epoxy/amine system, J. Appl. Polym. Sci. 124 (3) (2012) 1899–1905.
[40] C.C. Riccardi, R.J.J. Williams, A kinetic scheme for an amine-epoxy reaction with simultaneous etherification, J. Appl. Polym. Sci. 32 (2) (1986) 3445–3456.
[41] L. Chiao, R.E. Lyon, A fundamental approach to resin cure kinetics, J. Compos. Mater. 24 (7) (1990) 739–752.
[42] L. Chiao, Mechanistic reaction kinetics of 4,4'-diaminodiphenylsulfone cured tetraglycidyl-4,4'-diaminodiphenylmethane epoxy resins, Macromolecules 23 (5) (1990) 1286–1290.
[43] K.C. Cole, A new approach to modeling the cure kinetics of epoxy amine thermosetting resins. 1. Mathematical development, Macromolecules 24 (11) (1991) 3093–3097.
[44] K.C. Cole, J.-J. Hechler, D. Nöel, A new approach to modeling the cure kinetics of epoxy amine thermosetting resins. 2. Application to a typical system based on Bis [4-(diglycidylamino)phenyl]methane and Bis(4-aminophenyl) Sulfone, Macromolecules 24 (11) (1991) 3098–3110.
[45] J. Mijovic, A. Fishbain, J. Wijaya, Mechanistic modeling of epoxy-amine kinetics. 1. Model compound study, Macromolecules 25 (2) (1992) 979–985.
[46] J. Mijovic, A. Fishbain, J. Wijaya, Mechanistic modeling of epoxy-amine kinetics. 2. Comparison of kinetics in thermal and microwave fields, Macromolecules 25 (2) (1992) 986–989.
[47] N.A. St John, G.A. George, Cure kinetics and mechanisms of a tetraglycidyl-4,4'-diaminodiphenylmethane/diaminodiphenylsulphone epoxy resin using near i.r. spectroscopy, Polymer 33 (13) (1992) 2679–2688.
[48] E. Girard-Reydet, C.C. Riccardi, H. Sautereau, J.-P. Pascault, Epoxy-aromatic amine diamine kinetics. 1. Modelling and influence of the diamine structure, Macromolecules 28 (23) (1995) 7599–7607.
[49] M. Opalički, J.M. Kenny, L. Nicolais, Cure kinetics of neat and carbon-fiber reinforced TGDDM/DDS epoxy systems, J. Appl. Polym. Sci. 61 (6) (1996) 1025–1037.
[50] C.C. Riccardi, F. Fraga, J. Dupuy, R.J.J. Williams, Cure kinetics of diglycidylether of bisphenol A-ethylenediamine revisited using a mechanistic model, J. Appl. Polym. Sci. 82 (9) (2001) 2319–2325.
[51] L. Shechter, J. Wynstra, R.P. Kurkjy, Glycidyl ether reactions with amines, Ind. Eng. Chem. 48 (1) (1956) 94–97.
[52] I.T. Smith, The mechanism of the crosslinking of epoxide resins by amines, Polymer 2 (C) (1961) 95–108.
[53] K. Horie, H. Hiura, M. Sawada, I. Mita, H. Kambe, Calorimetric investigation of polymerization reactions. III. Curing reaction of epoxides with amines, J. Polym. Sci. A1 8 (6) (1970) 1357–1372.
[54] C.W. Wise, W.D. Cook, A.A. Goodwin, Chemico-diffusion kinetics of model epoxy-amine resins, Polymer 38 (13) (1997) 3251–3261.
[55] D. Lahlali, M. Naffakh, M. Dumon, Cure kinetics and modelling of an epoxy resin cross-linked in the presence of two different diamine hardeners, Polym. Eng. Sci. 45 (12) (2005) 1581–1589.
[56] N. Lahlali, J. Dupuy, M. Dumon, Tuning morphologies of thermoset/thermoplastic blends. Part 1: kinetic modelling of epoxy-amine reactions using amine mixtures, E-Polymers 6 (1) (2006) 1–12.
[57] N. Lahlali, J. Dupuy, M. Dumon, Tuning morphologies of thermoset/thermoplastic blends. Part 2: phase separation of poly(vinyl methylether), PVME, using amine mixtures as thermoset hardeners, E-Polymers 6 (2) (2006) 1–12.
[58] M. Romero, X. Fernandez-Franco, X. Ramis, Sequential heat release: an innovative approach for the control of curing profiles during composite processing based on dual-curing systems, Polym. Int. 68 (3) (2019) 527–545.

[59] U. Bandara, A systematic solution to the problem of sample background correction in DSC curves, J. Therm. Anal. 31 (1986) 1063–1071.
[60] J. Kim, T.J. Moon, J.R. Howell, Cure kinetic model, heat of reaction, and glass transition temperature of AS4/3501-6 graphite-epoxy prepregs, J. Compos. Mater. 36 (21) (2002) 2479–2498.
[61] D. Fylstra, L. Lasdon, J. Watson, A. Waren, Design and use of the microsoft excel solver, Interfaces 28 (5) (1998) 29–55.
[62] G. Voto, L. Sequeira, A.A. Skordos, Formulation Based Predictive Cure Kinetics Modelling of Epoxy Resins: Dataset, Cranfield Online Research Data Repository, 2021. https://doi.org/10.17862/cranfield.rd.14500809.
[63] Z. Man, J.L. Stanford, B.K. Dutta, Reaction kinetics of epoxy resin modified with reactive and nonreactive thermoplastic copolymer, J. Appl. Polym. Sci. 112 (4) (2009) 2391–2400.
[64] M. Akay, J.G. Cracknell, Epoxy resin-polyethersulphone blends, J. Appl. Polym. Sci. 52 (5) (1994) 663–688.
[65] G. Cracknell, M. Akay, Kinetics of curing reactions for epoxy-amine/polyethersulphone resins, J. Therm. Anal. 40 (2) (1993) 565–573.
[66] B. Fernández, M.A. Corcuera, C. Marieta, I. Mondragon, Rheokinetic variations during curing of a tetrafunctional epoxy resin modified with two thermoplastics, Eur. Polym. J. 37 (9) (2001) 1863–1869.

2021-10-26

Formulation based predictive cure kinetics modelling of epoxy resins

Voto, Gabriele

Elsevier

Voto G, Sequeira L, Skordos AA. (2021) Formulation based predictive cure kinetics modelling of epoxy resins. Polymer, Volume 236, November 2021, Article number 124304
https://doi.org/10.1016/j.polymer.2021.124304